The Polyborane, Carborane, Carbocation Continuum: Architectural Patterns

ROBERT E. WILLIAMS

Donald P. and Katherine B. Loker Hydrocarbon Research Institute, University of Southern California, Los Angeles, California 90089-1661

Contents

I. Introduction

Prior to the 1950s, most chemical compounds could easily be illustrated in two dimensions. Few papers dealt with clusters, particularly electron-deficient clusters, where three-dimensional renditions are virtually mandatory.

With the burgeoning of boron hydride, nonclassical carbocation, transition metal, and metallaorganic (aromatic hydrocarbon metal π complexes) chemistries, the literature has become progressively more involved in reporting electron-rich, electron-precise, and electron-deficient clusters. Today, one or two journals report on cluster compounds almost exclusively.

Most electron-precise and electron-rich clusters,[1] as they involve primarily two-center two-electron (2c2e) bonds, have expected connectivities and numerous isomers; electron-rich clusters also incorporate one-center two-electron (1c2e) lone pairs of electrons.

Our interest is in the electron-deficient clusters, and in particular the configurations and architectural features characteristic of the simplest and most abundant

Figure 1. Electrons, bonds, and connections in "N_2H_6", C_2H_6, and B_2H_6.

Figure 2. *arachno*-RSB_2H_5 and charge smoothing.

Robert E. Williams is currently a Senior Fellow of the Loker Hydrocarbon Research Institute (since 1979) and served as Associate Director of the Institute from 1984 to 1991. He obtained his Ph.D. from the University of New Mexico in 1952 and his B.A. from De Pauw University in 1948. From 1966 to 1969, he was Director of Research and Education at the Aerojet-General Corporation. In 1970, he founded Chemical Systems, Inc. in Irvine, CA and served as President until its acquisition by the Purolator Corporation in 1980. He pioneered the discovery and chemistry of the smaller compounds of carbon, boron, and hydrogen, called carboranes, and elucidated their structures. His geometrical systematization of the polyborane and carborane cluster compounds enabled others to generate the now-familiar electron-counting rules that apply to carbocations and inorganic and organometallic chemical cluster compounds in general. More recently, he has become involved in the theory, structure, and function of microporous filtration membranes. He has published numerous scientific papers, a number of chapters, and three books. Most recently, he was coeditor and coauthor of *Electron Deficient Boron and Carbon Clusters* published by Wiley-Interscience in 1991, was coauthor of *Hypercarbon Chemistry* published by Wiley-Interscience in 1987, and was editor and coauthor of *Advances in Boron and the Boranes* published by VCH in 1988.

electron deficient clusters, i.e., the structures of the polyborane, carborane, and carbocation continuum.[2] These continuum configurations constitute the primeval touchstone geometries of electron-deficient clusters to which other, more esoteric types of electron-deficient compounds may be related in fairly well-understood ways.

A. Electron-Deficient, Electron-Precise, and Electron-Rich Compounds

Electron-deficient compounds are those which have more valence orbitals than valence electrons or contain too few electrons to coordinatively saturate all skeletal atoms involving solely 2c2e bonds. Electron-deficient compounds are of two varieties: the first type incorporates 2c2e bonds only and leaves the borons or carbons under consideration coordinatively unsaturated; i.e., they have access to six valence electrons in three 2c2e bonds rather than access to an octet of electrons. Simple examples are trialkyl or trihalo boranes, BR_3 or BX_3, or the classical carbenium carbocations, R_3C^+.

The second category of electron-deficient compound involves multicenter bonding. In these cases, the skeletal atoms all have access to an octet of electrons but some of the bonding electron pairs are shared between three atoms (or four) in three-center two-electron, 3c2e, bonds (or 4c2e bonds). Examples of this second type include diborane, B_2H_6 (Figure 1), the dimer of trimethyl aluminum, Me_6Al_2, and the nonclassical 2-norbornyl carbocation, $C_7H_9^+$. Multicenter bonding may be extended beyond 4c2e bonds as a 12c2e mo-

lecular orbital may be considered to exist within *closo*-$B_{12}H_{12}^{2-}$.
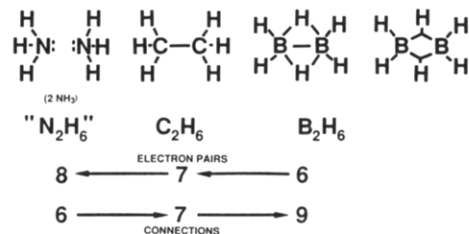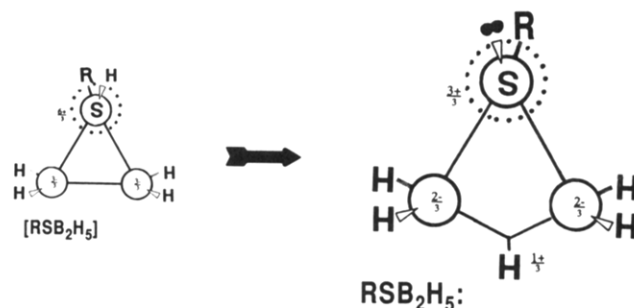
B. Less Electrons, More "Connections"

Structures involving pairs of boron, carbon, and nitrogen atoms coupled with six hydrogens are compared in Figure 1. By the early 1950s, it was accepted[3a] that fewer bonding electrons (greater electron deficiency) resulted in more "bonds". If we compare the numbers of electron pairs available for bonding in "N_2H_6", C_2H_6, and B_2H_6 (Figure 1) and change the word "bonds" to "connections" these trends are illustrated. For example, two nitrogens and six hydrogens produce two molecules of ammonia with six 2c2e bonds utilizing six of the eight electron pairs; two electron pairs reside as lone pairs on nitrogen (1c2e). In ethane, seven electron pairs are available for bonding and seven connections (or seven bonds) are formed.

Diborane, B_2H_6, is illustrated in two different ways; on the left, we draw lines connecting all atoms that are within bonding distance of one another (connections). There are nine connections, but there are only six electron pairs to make these nine connections, thus, two 3c2e bonds are required as illustrated at far right in Figure 1. The connections *increase* from six to seven to nine as the electron pairs available for making the connections *decrease* from eight to seven to six. Most of the illustrations in this article display connections rather than bonds.

C. Charge Smoothing

It is illustrative to compare two alternative tautomers for RSB_2H_5 (Figure 2). In the incorrect tautomer (left in Figure 2) the bonding is electron precise, the borons, hydrogens, and sulfur are all connected by 2c2e bonds. In this form, the sulfur has a strong positive charge in comparison to substantial negative charges on the two borons. In order to minimize these dipoles, a proton may be considered (hypothetically) to leave the sulfur and to relocate as a bridge hydrogen between the two borons to produce the correct structure (right in Figure 2). The driving force is charge smoothing. In this

Figure 3. Nido-compounds structurally related to B_6H_{10}.

fashion the positive charge on sulfur is greatly lessened, and the negative charges on the two borons are minimized.[3b]

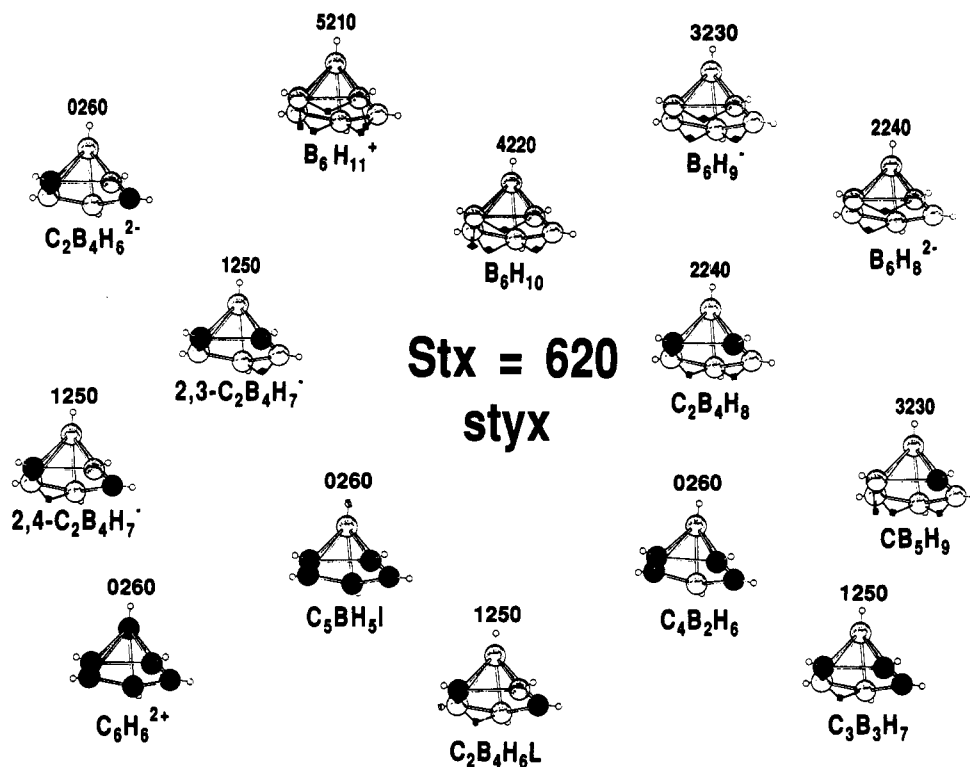In the correct structure (right in Figure 2) there are three regions, an electron-rich zone (the lone electron pair, 1c2e, on sulfur), an electron-precise region connecting the sulfur to the two borons (two 2c2e bonds), and an electron-deficient region involving the two borons and a bridging hydrogen (a 3c2e bond); electron rich does not mean negatively charged. Charge smoothing is one of the most important structural influences in fluxional electron-deficient compounds. The origin of the charges in Figure 2 are discussed in sections V and VI.

D. More 3c2e Bonds, Fewer Isomers

Diborane, B_2H_6 (Figure 1), incorporates two 3c2e bonds. All larger polyboranes involve many such multicentered bonds. Among the nonfused polyboranes, there are virtually no empirical formulae that give rise to more than one geometrical arrangement of boron atoms with three notable exceptions, i.e., two isomers apiece for the arachno-compounds, B_9H_{15}[4] and $B_6H_{11}^{-}$,[5a] and the randomly cocrystallized isomers of $B_9H_{13}^{2-}$ in the solid state (see section IX.H.). The absence of isomers may be attributed to inherent fluxionality occasioned by the presence of numerous 3c2e bonds which in turn allow clusters of borons and hydrogens to rearrange easily into their thermodynamically and geometrically most stable configurations.

This same tendency is somewhat lessened among the carboranes which geometrically resemble the polyboranes closely, but include carbons substituting for various borons within their structures. In the neutral carboranes, there are frequently several isomers; 3c2e bonds are less numerous in carboranes than in comparable neutral polyboranes, decreasing by one 3c2e bond

for each boron replaced by carbon. Generally, carborane isomers involve different locations of the carbons among otherwise equivalent sites on quite similar deltahedral or deltahedral fragment geometries.

In contrast to the polyboranes and carboranes, more geometrical isomers per empirical formula are found among the carbocations.[5b] Perhaps this reflects the fact that most nonclassical carbocations involve only one 3c2e bond per carbocation.

The aforementioned electron-deficient carboranes, polyboranes, and carbocations are quite different from comparable electron-precise compounds of which neutral hydrocarbons are but one example. One can easily imagine a dozen or so isomeric aliphatic hydrocarbons with six carbons and 10 hydrogens, i.e., C_6H_{10}; whereas in contrast, only one isomer of $nido$-B_6H_{10} is observed (Figure 3). The styx and Stx identification numbers in Figure 3 will be explained in section III.

II. Empirical Formula and Skeletal-Electron-Counting Classifications

All electron-deficient neutral continuum compounds are related to the following four classes and are identified by the four general formulae, $closo$-$C_{0\,to\,2}B_nH_{n+2}$, $nido$-$C_{0\,to\,4}B_nH_{n+4}$, $arachno$-$C_{0\,to\,6}B_nH_{n+6}$, and $hypho$-$C_{0\,to\,8}B_nH_{n+8}$. The subscript n refers to the number of boron atoms. The addition of one or more protons to the four general formulae produces cations while the abstraction of one or two protons from the four general formulae produces anions and dianions. Since the number of skeletal electrons (the sum of Lipscomb's styx numbers[6–8]) does not change upon the addition or abstraction of protons, the class does not change.

It follows that the $closo$-class, $C_{0\,to\,2}B_nH_{n+2}$ includes closo-neutral species such as $C_2B_3H_5$ (where n = 3) to $C_2B_{10}H_{12}$ (n = 10) and CB_5H_7 (where n = 5), as well as many closo-anions such as $CB_{11}H_{12}^{-}$ (n = 11), and of
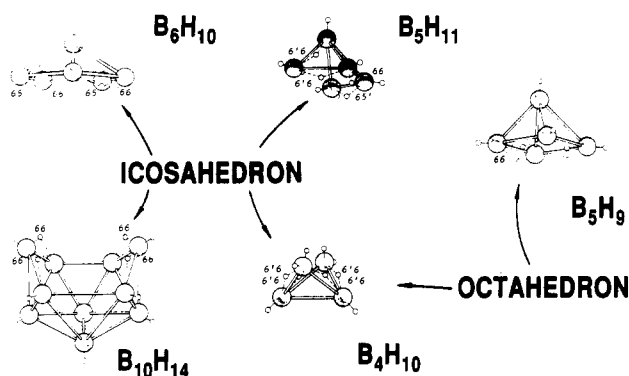
Figure 4. Polyboranes related to the icosahedron and the octahedron.

course the many closo-dianions, $B_6H_6^{2-}$ to $B_{12}H_{12}^{2-}$. Of course, one and two protons are abstracted from the general formulae in these cases to incorporate anions, $C_{0\,to\,1}B_nH_{n+1}^-$, and to incorporate dianions, $B_nH_n^{2-}$. Similar modifications are applicable to the nido-, arachno-, and hypho-classes also.

The skeletal electrons vary monotonically from class to class, $2n + 2$ skeletal electrons characterizing the closo-compounds, $2n + 4$ the nido-species, $2n + 6$ the arachno-species, and $2n + 8$ electrons the hypho-compounds (n in the case of skeletal-electron counting refers to the total number of skeletal framework atoms, i.e. borons, carbons, nitrogens, etc.).

There are many reasons that selected neutral hydrocarbons should be considered as members of the continuum and several reasons most hydrocarbons should not be included. Neutral and negatively charged hydrocarbons are considered beyond the scope of the present article.
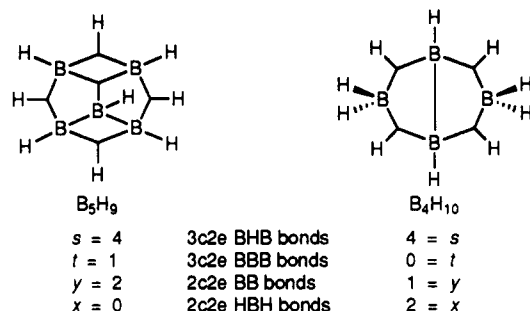
III. Concentric Spheres Model and Chop-Stx Nomenclature

One of Lipscomb's seminal contributions[6] to the understanding of polyborane or boron hydride chemistry was to consider separately "the more diagnostic" skeletal atoms and skeletal electron pairs from "the less informative" exo-terminal atoms and exo-terminal electron pairs. He viewed the atoms in the various deltahedral and deltahedral fragment structures to be radially disposed about the vertices of two concentric spheres. His preference at the time was for spheres that enclosed the vertices of the regular icosahedron or octahedron (Figure 4) and he generated the deltahedral fragment structures by removing neighboring vertices from the icosahedron (usually) and the octahedron (rarely). The numbers in Figure 4 (66 and 65, etc.) identify the coordination numbers of the two borons associated with each bridge hydrogen and will be discussed in section VI.B.

On the surface of the inner sphere, Lipscomb placed the skeletal borons and carbons as well as the skeletal hydrogens (i.e., the bridge and endo-hydrogens) as well as the skeletal electron pairs that held them together. On the outer sphere, he located the various exo-terminal groups (i.e. the exo-terminal hydrogens, alkyl groups, Lewis bases, etc.). The terminal electron pairs were identified as those that attached the exo-terminal groups (on the outer sphere) to the skeletal borons and carbons (inner sphere).

The skeletal electron pairs were further assigned to various kinds of 2c2e and 3c2e bonds. Lipscomb cataloged these skeletal bonds under the very informative styx format (the number above each structure in Figure 3) wherein s stands for the number of bridge hydrogens or skeletal BHB (3c2e) bonds, t stands for the skeletal BBB (3c2e) bonds, y equals the skeletal BB (2c2e) bonds, and the x stands for the endo hydrogen (2c2e) bonds of BH_2 groups. The bonds connecting exo-terminal groups are not identified.

Examples of Lipscomb's styx labeling applied to nido-B_5H_9 and arachno-B_4H_{10} follow:

B_5H_9		B_4H_{10}
$s = 4$	3c2e BHB bonds	$4 = s$
$t = 1$	3c2e BBB bonds	$0 = t$
$y = 2$	2c2e BB bonds	$1 = y$
$x = 0$	2c2e HBH bonds	$2 = x$

We strongly favor an abbreviated form of Lipscomb's styx systematics[6] which we call "Chop-Stx".[2] In converting from "Lip-styx" to Chop-Stx, we notionally "chop off" the bridging hydrogens from the s BHB (3c2e) bonds which allows them to be added to the y BB (2c2e) bonds. Thus, the s BHB bonds plus the y BB bonds appear under the symbol S ($s + y = S$). In this fashion, it becomes immaterial whether a given BB bond pair of electrons is also associated with a bridging hydrogen or not. As both the Chop-Stx and styx systematics must be used in conjunction with the empirical formula, no information is lost. The difference between the total number of hydrogens and terminal groups in the empirical formula and the number of heavy skeletal atoms yields the number of "extra" skeletal hydrogens that must be found either as bridge or as endo-hydrogens. Since the x in Chop-Stx reveals how many of the extra skeletal hydrogens are endo-hydrogens, the balance must always be bridge hydrogens.

The advantage of Chop-Stx is that, under one easily remembered Stx number, we can now identify all compounds that are isoelectronic with a given polyborane. For example, in Figure 3 are shown a variety of styx numbers above each of the myriad of compounds that are isoelectronic and isostructural with B_6H_{10}. All of these compounds with their seemingly unrelated styx numbers, fall under the single, easily remembered Chop-Stx label, 620, in the center of Figure 3. Lipscomb's original styx number,[6] if desired, may be reconstructed in seconds by simply comparing the Chop-Stx number with the empirical formula.

In Figure 5 are illustrated a catalog of simplified Chop-Stx numbers that covers all known polyboranes, carboranes, and carbocations as well as some neutral hydrocarbons. Throughout the figures, the three digit Chop-Stx number will usually be found accompanying most structural illustrations.

IV. Geometrical Systematics

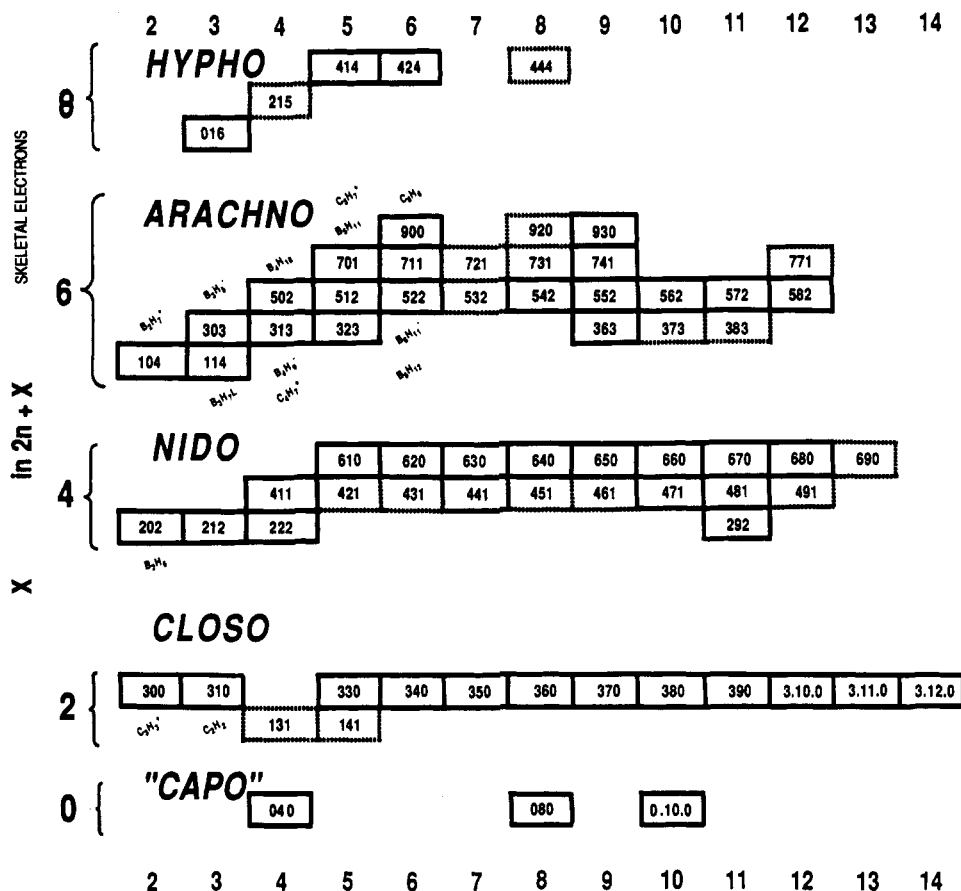In the 1950s and -60s, it was thought that all polyboranes could be viewed as having structures resem-

Figure 5. Chop-Stx cataloging of the polyborane–carborane–carbocation continuum.

bling fragments of the regular icosahedron (Figure 4), except for B_5H_9, whose structure was derived from a regular octahedron. As the series of most spherical closo-carboranes, $C_2B_nH_{n+2}$, and closo-$B_nH_n^{2-}$ dianions were discovered (left hand column of Figure 6), the primitive icosahedral viewpoint lost its sanctity.

A. Most-Spherical[2,8,9] Deltahedra and Their Fragments

In 1971, Williams pointed out[9] that the known series of deltahedral[10a] fragments, characteristic of nido-polyboranes, nido-carboranes, and the nido-carbocation, $C_5H_5^+$, could almost always be derived from the unique series of most-spherical[2,8,9] closo-deltahedra (with 6–12 vertices) by the removal of one high-coordinated vertex from each deltahedron and that the arachno-deltahedral fragments could subsequently be derived (from the nido-fragments) by the removal of one additional high-coordinated vertex neighboring the open faces. The most spherical deltahedra are always those with the most uniformly or most homogeneously connected vertices and will be discussed below in section V.A. and illustrated in Figure 14.

The original geometrical systematics[9] have been expanded to include both larger and smaller deltahedra (with 5–14 vertices) as illustrated in Figure 6. Representative compounds with the deltahedral fragment structures anticipated in Figure 6 have been found, perhaps even the anticipated arachno-7-vertex configuration. The predicted nido-13- and arachno-12-vertex structures derived by dissecting the most-spherical

closo-14-vertex deltahedron have not been confirmed. Discussion of Shore's[5a,10b,10c] arachno-$B_7H_{12}^-$ and its adduct with $Fe(CO)_4$ is discussed in section IX.F.

Throughout the text and in Figure 6, we identify the various deltahedra and their fragments with terms such as ni-5⟨IV⟩ which indicates a nido-5-vertex structure with a tetragonal (or IV-gonal) open face, e.g., B_5H_9 in Figure 4. It is derived by removing one four-connected (4 k) vertex from the closo-6-vertex deltahedron (octahedron) whose largest aperture is a triangle or III-gon (clo-6⟨III⟩). The term ni-12⟨VI+i⟩ in Figure 6 identifies a nido-deltahedral fragment derived from the clo-13⟨III⟩ deltahedron by the removal of one six-connected (6 k) vertex producing a VI-gonal open face plus the additional removal of one additional connection ⟨i⟩ (away from the open face) which eliminates the other 6 k vertex and generates another tetragonal face.

The solid arrows in Figure 6 relate species that differ by the removal of one high-coordinated vertex while broken arrows identify the removal of lower coordinated vertices. Wavy lines relate structures that differ by one connection.

The enlarged structures in Figure 6 are those observed with boron–carbon–hydrogen skeletal atoms while the reduced-scale structures are those observed when four-skeletal-electron-donor heteroatoms or selected transition element groups are incorporated.

The 1971 geometrical systematics[9] were deliberately restricted to the consideration of closo-deltahedra with 6–12 vertices as some concern was raised about the probable geometry of electron-deficient nido-4-vertex compounds. Twenty years later, we feel comfortable extending the systematics to include both larger, 13-
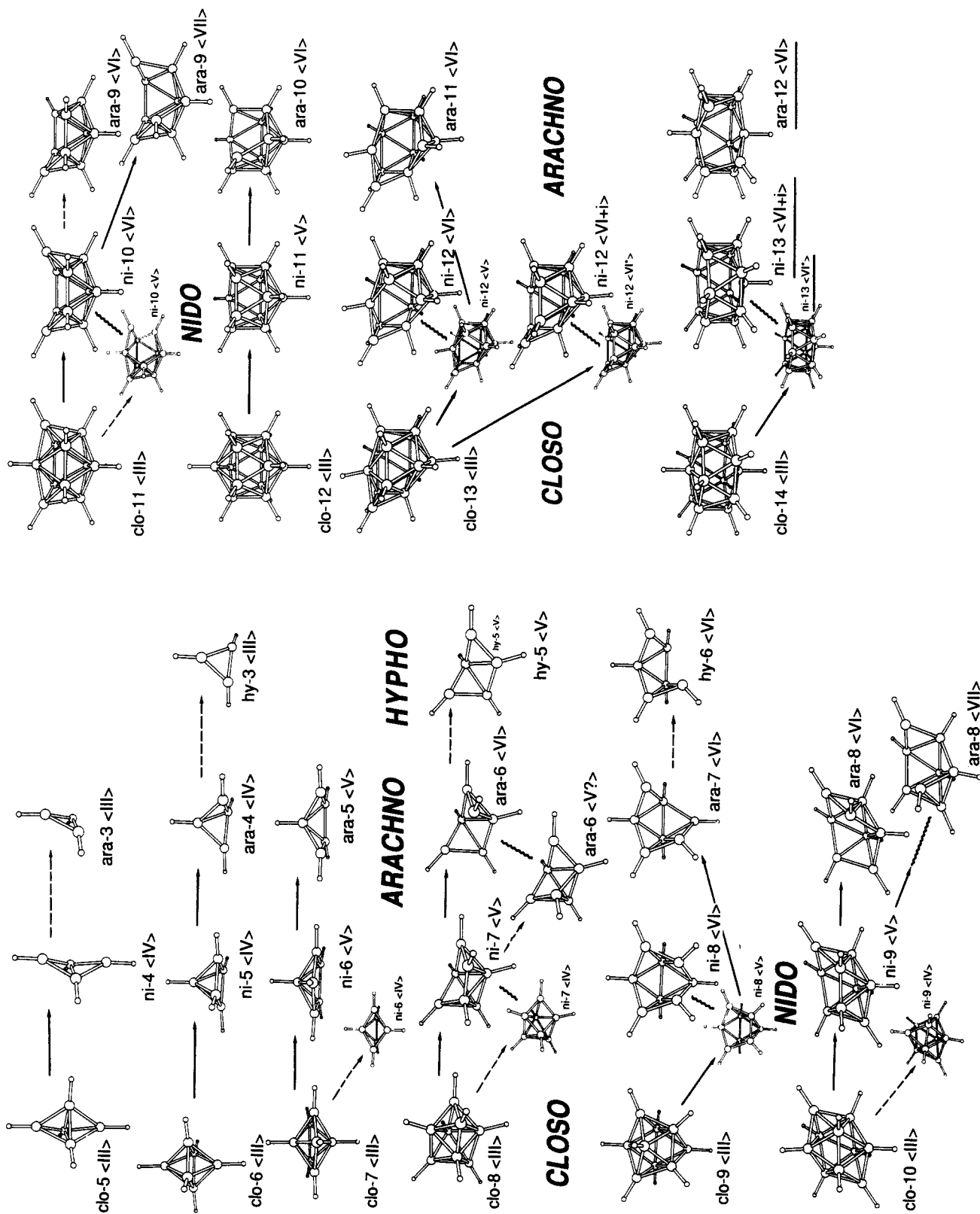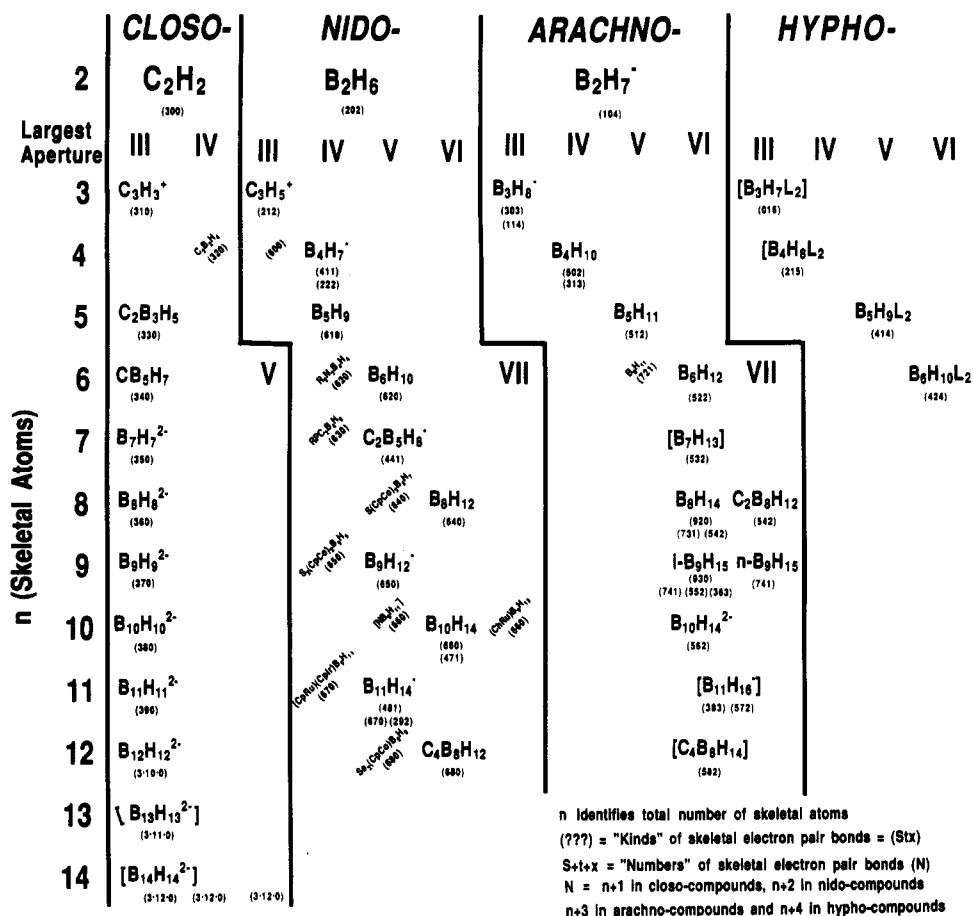
Figure 6. Geometrical systematics (1991).

	CLOSO-	NIDO-	ARACHNO-	HYPHO-
2	C_2H_2	B_2H_6	$B_2H_7^-$	
	(300)	(202)	(104)	
Largest Aperture	III IV	III IV V VI	III IV V VI	III IV V VI
3	$C_3H_3^+$ (310)	$C_3H_5^+$ (212)	$B_3H_8^-$ (303)(114)	$[B_3H_7L_2]$ (016)
4	C_4H_4 (...)	$B_4H_7^-$ (411)(222)	B_4H_{10} (502)(313)	$[B_4H_6L_2$ (215)
5	$C_2B_3H_5$ (330)	B_5H_9 (610)	B_5H_{11} (512)	$B_5H_9L_2$ (414)
6	CB_5H_7 (340) V	B_6H_{10} (620) VII	B_6H_{12} (522) VII	$B_6H_{10}L_2$ (424)
7	$B_7H_7^{2-}$ (350)	$C_2B_5H_6^-$ (441)	$[B_7H_{13}]$ (532)	
8	$B_8H_8^{2-}$ (360)	B_8H_{12} (640)	B_8H_{14} (920)(731)(542) $C_2B_6H_{12}$ (542)	
9	$B_9H_9^{2-}$ (370)	$B_9H_{12}^-$ (650)	$i\text{-}B_9H_{15}$ (930)(741)(552)(363) $n\text{-}B_9H_{15}$ (741)	
10	$B_{10}H_{10}^{2-}$ (380)	$B_{10}H_{14}$ (660)(471)	$B_{10}H_{14}^{2-}$ (562)	
11	$B_{11}H_{11}^{2-}$ (390)	$B_{11}H_{14}^-$ (481)(670)(292)	$[B_{11}H_{16}^-]$ (383)(572)	
12	$B_{12}H_{12}^{2-}$ (3-10-0)	$C_4B_8H_{12}$ (680)	$[C_4B_8H_{14}]$ (582)	
13	$[B_{13}H_{13}^{2-}]$ (3-11-0)			
14	$[B_{14}H_{14}^{2-}]$ (3-12-0)(3-12-0)(3-12-0)			

n (Skeletal Atoms)

n Identifies total number of skeletal atoms
(???) = "Kinds" of skeletal electron pair bonds = (Stx)
S+t+x = "Numbers" of skeletal electron pair bonds (N)
N = n+1 in closo-compounds, n+2 in nido-compounds
n+3 in arachno-compounds and n+4 in hypho-compounds

Correlation of Skeletal Atoms and Skeletal Electrons with Aperture Size

Figure 7. Examples of compounds that subscribe to the various geometries of Figure 6 and their Stx numbers of Figure 5.

and 14-vertex, and smaller, 5-vertex, closo-deltahedra. Nido-deltahedral fragments with 4–13 vertices and arachno-fragments with 3–12 vertices are also illustrated in Figure 6.

The geometrical pattern reported in 1971 suggested that the preferred nido-deltahedral fragment structures for boron–carbon–hydrogen clusters would *always* be produced following the removal of the *highest* coordinated vertex from each of the most-spherical closo-deltahedra. The 1971 empirical rule is still correct with one exception; in generating the preferred nido-8-vertex fragment from the closo-9-vertex deltahedron (when the skeletal atoms are composed solely of boron, carbon, and hydrogen) we note (empirically) that one additional high-coordinated edge connection, $\langle i \rangle$, must also be removed[11] to yield a VI-gonal open face rather than the V-gonal open face.

We now add a new corollary to cover the dissection of 13- and 14-vertex deltahedra which incorporate two nonadjacent 6 k vertices. The removal of one highest coordinated 6 k vertex will not lower the connectivity of the other 6 k vertex, but the removal of selected 5 k vertices will reduce both 6 k vertices to 5 k vertices simultaneously!

The 13-vertex closo-deltahedron (clo-13$\langle III \rangle$) contains two nonadjacent 6 k vertices. The removal of one 6 k vertex (old rule) leaves the other offensive 6 k vertex untouched in the resulting nido-deltahedral fragment (ni-12$\langle VI* \rangle$). Such 6 k vertices are apparently intolerable in nido-compounds that only incorporate boron, carbon, and hydrogen in their skeletons. The asterisk

indicates the presence of the remaining 6 k vertex (illustrated in Figure 6).

In contrast, when an appropriate transition element group is present, it can occupy the remaining offensive 6 k vertex, and the nido-fragment retaining one 6 k vertex (ni-12$\langle VI* \rangle$) is actually the preferred structure.[2,12]

To eliminate both offensive 6 k vertices simultaneously, in the closo-13-vertex deltahedron, one of the two specific 5 k vertices that are connected to both 6 k vertices must be selected for removal (new corollary). The removal of one of these specific 5 k vertices simultaneously reduces the connectivity of both of its neighboring 6 k vertices to 5 k vertices in the resulting 12-vertex nido-deltahedral fragment (ni-12$\langle V \rangle$) as is illustrated in Figure 6. One additional connection, $\langle i \rangle$, must also be removed when the nido-12-vertex skeletons are composed solely of boron, carbon, and hydrogen, which results in the two configurations, ni-12$\langle VI \rangle$ and ni-12$\langle VI+i \rangle$, which have been observed. The initial ni-12$\langle V \rangle$ configuration is observed when one or two four-skeletal-electron-donor heteroatoms are present (see below).

All nido-configurations have tetragonal, pentagonal, or hexagonal open faces (Figure 6). Roman numerals are used to identify the sizes of the open faces; for example, nido-B_5H_9 has a IV-gonal open face, and nido-B_6H_{10} (Figures 3 and 4) has a V-gonal open face while nido-$B_{10}H_{14}$ has a VI-gonal open face. Examples relating preferred open-face geometries and Chop-Stx numbers are illustrated in Figure 7.
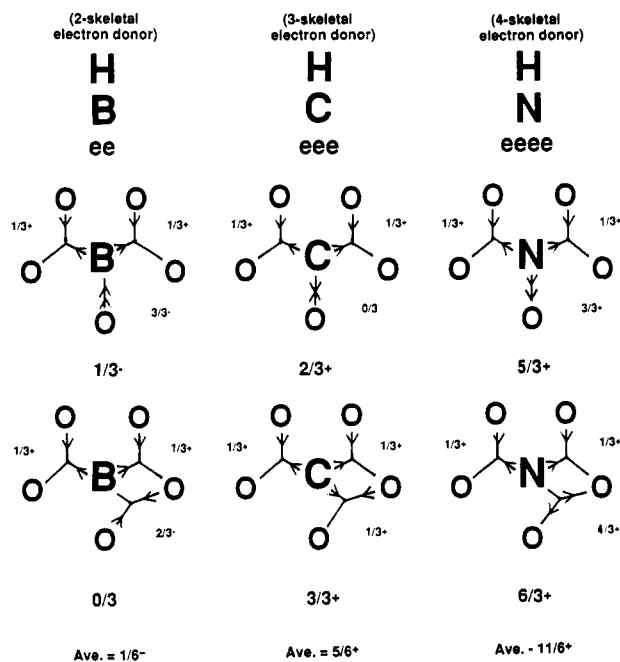
Figure 8. Residual charges on the two-, three-, and four-skeletal-electron donors, B, C, and N in possible bond networks.

B. Structural Responses to Heteroatom Substitution in *closo*-, *nido*-, and *arachno*-Polyborane Structures

In polyborane structures, each neutral BH group contributes two electrons to the number of skeletal electrons (borons are two-skeletal-electron donors). Neutral CH groups are three-skeletal-electron donors when they are substituting for BH groups (carboranes) while neutral NH groups substituting for BH groups (azaboranes) are four-skeletal-electron donors. Each boron, carbon, and nitrogen contributes an additional electron to the exo-terminal hydrogen bond, but as far as skeletal-electron donation is concerned, the boron, carbon, and nitrogen atoms are two-, three-, and four-skeletal-electron donors, respectively.

Against a background of polyborane skeletons and their anions and dianions composed solely of borons (two-skeletal-electron donors) and hydrogens, plus or minus additional electrons as required, how do carbons (three-skeletal-electron donors) and nitrogens (four-skeletal-electron donors) influence the electron distributions when one or more are substituted for skeletal borons? Comparative examples would be $closo$-$B_{10}H_{10}^{2-}$ versus $closo$-$C_2B_8H_{10}$ versus $closo$-NB_9H_{10}, and $nido$-$C_4B_2H_6$ versus $nido$-$N_2B_4H_6$, and $arachno$-$B_9H_{13}^{2-}$ versus $arachno$-$C_2B_7H_{13}$ versus $arachno$-NB_8H_{13}.

Our assumptions about the donation of electrons to match the skeletal-electron requirements indicate that the boron atom donates two skeletal electrons to the deltahedron while the carbon atom donates three skeletal electrons and the nitrogen atom donates four electrons to the skeleton. As a result the nitrogen has the highest positive field around it, the carbon is next, and the boron has the lowest "positive" field.

Consider each of the 12 equivalent BH groups in $closo$-$B_{12}H_{12}^{2-}$ (left hand column in Figure 8; B = BH groups and circles = five neighboring borons); the borons contribute three electrons, one to the exo-terminal

Consequences of Substituting 3-skeletal electron donors (eg. carbon) and 4-skeletal electron donors (eg. nitrogen) for 2-skeletal electron donors (eg. boron):

	Closo-			Nido-			Arachno- & Hypho-		
	B	C	N	B	C	N	B	C	N
Preempt Low Coordination Vertices	-	+	+	-	+	+	-	+	+
Avoid Neighboring Bridge Hydrogens	-	+	+	-	+	+	-	+	+
Increase Virtual Electron Deficiency and Connectivity (∴ Smaller Apertures)				-	-	+			
Avoid Neighboring Endo Hydrogens							-	±	+

Figure 9. Accommodation of three- and four-skeletal-electron-donor heteroatoms as a function of class.

hydrogen and two to the total skeletal electron count. As closo-compounds require $2n + 2$ skeletal electrons, two additional electrons must be added which account for the 2– charge. The borons under consideration are illustrated at the left of Figure 8 in the two possible environments in $closo$-$B_{12}H_{12}^{2-}$ involving either three 3c2e bonds (bottom) or two 3c2e bonds and one 2c2e bond (top).

For simplicity, if the boron atom is arbitrarily assumed to donate its two skeletal electrons to two 3c2e bonds, it accumulates two $1/3$+ charges. On the other hand, to gain access to an octet of electrons, the boron receives either $3/3$– charge donated from a neighboring boron via a 2c2e bond (top) or $2/3$– charge donated from two neighboring borons via a 3c2e bond (bottom). These two situations result in an oversimplified net charge on each BH group of either $1/3$– or $0/3$– (which averages $1/6$–). In fact, the 2– charge divided by 12, for $B_{12}H_{12}^{2-}$, results in $1/6$– charge per BH group. Similar treatment of CH and NH groups substituting for BH groups and assuming identical skeletal-electron distributions (possible bond networks) leads to average charges of $5/6$+ on the carbon and to $11/6$+ on the nitrogen.

It is reasonable to assume that the carbon and to a much greater extent the nitrogen would tend to preempt 2c2e "bonds" and to avoid 3c2e rich environments (thus favoring the top illustrations in Figure 8), but they would still have roughly $2/3$+ and $5/3$+ charges in such possible bond networks. Charge-smoothing forces, augmented by greater electronegativity, would be expected to inductively displace the skeletal-electron distributions toward the positively charged NH group and two CH groups and therefore away from the remaining $B_{11}H_{11}$ and $B_{10}H_{10}$ moieties in both $HNB_{11}H_{11}$[13] and $H_2C_2B_{10}H_{10}$.

The BH environments in $HNB_{11}H_{11}$ and $H_2C_2B_{10}H_{10}$ would thus become incrementally more electron deficient compared to the situation in the parent $closo$-$B_{12}H_{12}^{2-}$. Incrementally increased electron deficiency would be expected to favor an increase in the numbers of connections (see section I.B. and Figure 1) in susceptible systems. Increasing the numbers of connections is not possible in closo-deltahedra but has been observed in many nido-systems (see Figure 9).

Exceeding the scope of this review, incrementally lowered electron deficiency, larger apertures, and less connections result when groups donating 0 to –2 skeletal

electrons to the nido-skeletal-electron pool are incorporated. Nido-fragments of different deltahedra than those illustrated in Figure 6 are involved in such cases (see Summary, section XII).

In all three classes (closo, nido, and arachno) the carbons and nitrogens, having made larger contributions to the total number of skeletal electrons, as compared to the borons, inductively attract the skeletal electrons toward the carbons and nitrogens and away from the borons with the following four consequences.

First, in the competition for electron density (and to maximize charge smoothing) the carbons *usually* (in the most stable isomers) and the nitrogens *always* seek out and occupy the lowest connected electron rich vertices geometrically available within all three closo-, nido-, and arachno-classes.

Second, when four-skeletal-electron donors (RN, :S) replace two-skeletal-electron donors (HB) and inductively attract more electron density to themselves, the rest of the cage becomes incrementally more electron deficient. In section I.B. (Figure 1) it was pointed out that greater electron deficiency engenders a greater number of connections. In this fashion, the substitution of four-skeletal-electron donors for two-skeletal-electron donors incrementally increases the electron deficiency, which in turn results in more connections and smaller apertures when such optional structures are available.

Third, identically connected vertices in deltahedral fragments with smaller open faces, have greater electron density associated with those vertices than if such identically connected vertices were incorporated into alternative deltahedral fragments with larger open faces (for details, see ref 1).

In closo-compounds, the carbons and nitrogens can seek out lowest connected electron-rich vertices (first consequence above), but there can be no increase in the number of connections, and thus no apertures that can be made smaller in order to produce a more tightly knit deltahedron. It follows that the second consequence and third consequence are inapplicable to closo-compounds. In the nido-compounds, however, different deltahedral fragment structures (with an additional connection and smaller apertures) are frequently adopted primarily to accommodate incrementally greater electron deficiency and, on occasion, to sate nitrogen's (four-skeletal-electron donor) greater need for electron density. Carbon's (three-skeletal-electron donor) influence and/or need is usually not sufficient to effect such changes in shape.

Fourth, there is a sharp difference between most nido- and arachno-compounds in the manner of accommodating carbon's and nitrogen's greater "need" for electron-rich environments. *arachno*-Polyboranes usually (but not always) incorporate BH_2 groups with one or two neighboring bridge hydrogens involving 3c2e bonds (H_2B-H- or $H_2B(-H-)_2$ groups). Carbons, when substituting for borons, tend to preempt such positions and to become CH_2 groups, but except in two carborane cations at low temperature, no bridge hydrogens are ever found adjacent to such CH_2 groups. Avoiding adjacent bridge hydrogens results in lower coordination to carbon, fewer 3c2e bonds, and less sharing of electrons by the carbon.

Nitrogens might be imagined (incorrectly) to preempt such locations also, and to hypothetically produce NH_2

groups without neighboring bridge hydrogens and their 3c2e bonds, but in fact, such imaginary NH_2 groups apparently are not favored as they normally jettison their endo-protons (even less electron sharing) and form NH groups of even lower coordination number. The jettisoned imaginary endo-protons either leave the molecule entirely, producing anions, or relocate on remote BB bonds to form BHB bridge hydrogens. Apparently the nitrogen retains the endo-lone pair of electrons on nitrogen as well as the exo-terminal hydrogen (see also section I.B. and Figure 1, where sulfur in RSB_2H_5[14] may be imagined to lose an endo-proton to a remote BB bond while it retains the lone pair of electrons on sulfur).

In summary, nitrogen, when substituting for boron, always occupies a site with the smallest number of connections *available*; however, the nitrogen is (a) forced to "tolerate" the boron-preferred shape when impressed into closo-deltahedra, but (b) will be shown to cause the assumption of a deltahedral fragment shape, with one more connection, when incorporated into most nido-compounds (the nitrogen still assumes a lowest connected site *available*, usually, but not always, of equivalent connectivity), and (c) will be shown to jettison what would otherwise become endo-hydrogens on nitrogen when incorporated into arachno-compounds. These last two strategies are the result of nitrogen's effort to inductively attract some of the four-skeletal-electron donation it contributed toward the total number of skeletal electrons. Charge smoothing is the underlying driving force.

These two differences (b and c above) in accommodating three- and four-skeletal-electron-donor heteroatoms (Figure 9) illustrate why quite different approaches are required in discussing nido-compounds[2] (where different shapes are frequently adopted and endo-hydrogens are generally absent) and arachno-compounds (where endo-hydrogens are usually present on boron, are labile on carbon, and are jettisoned from nitrogen).

The configurations of the *closo*-, *nido*-, *arachno*-, and *hypho*-polyboranes, -carboranes, and -carbocations, incorporating only boron, carbon, and hydrogen, should be considered the simple, primeval touchstone geometries of electron-deficient-cluster chemistry. Alternative geometrical shapes and varying endo-bridge hydrogen ratios, when heteroatoms are incorporated, should be deemed special cases and their somewhat different structures can usually be simply related to the primeval configurations of the aforementioned continuum of boron–carbon compounds in an empirically defined manner (Figure 6).

C. Procedure for Elucidating the Architectural Patterns of the *closo*-, *nido*-, *arachno*-, and *hypho*-Polyboranes, -Carboranes, and -Carbocations

In light of the concepts thus far reviewed, an effort will be made to account for the (a) known, (b) proposed, (c) "thought-to-be", and (d) "by-default-must-be" structures assigned to the various closo-, nido-, arachno-, and hypho-compounds.

It is useful to relate the various classes with the presence of various architectural features (Figure 10) prior to discussing them in the following sections. The

Figure 10. Architectural features common to various classes.

identification of the endo-terminal skeletal hydrogens of BH_2 groups (or terminal hydrogens on the inner sphere) as opposed to the exo-terminal hydrogens of the same BH_2 groups (or terminal hydrogens on the outer sphere) are illustrated in Figure 4 in the cases of arachno-B_4H_{10} and arachno-B_5H_{11}. In cases like nido-B_2H_6 and arachno-$B_3H_8^-$ (Figures 1 and 29–31) the endo and exo assignments are completely arbitrary and in each BH_2 group one hydrogen is assigned as an exo-hydrogen and the other as an endo-terminal hydrogen for book-eeping purposes only.

Closo-compounds are almost exclusively constructed about the vertices of closed deltahedra (Figure 6). In only one or two cases are bridge hydrogens involved. Such rare bridge hydrogens on closo-deltahedra, as in CB_5H_7[15] and $B_6H_7^-$,[6] are probably attached to the boron skeletal atoms by 4c2e bonds over triangular faces.

The closo-configurations are convenient for assessing the electron distributions in both closo- and nido-configurations and the anticipation of carbon location isomers within the closo-carboranes as a function of electron distribution.

Nido-configurations have deltahedral fragment structures with tetragonal (IV-gonal), pentagonal (V-gonal), and hexagonal (VI-gonal) open faces. Electron distributions will be extrapolated from closo-deltahedra and applied to the nido-clusters.[2]

There are a few unusual nido-compounds that incorporate BH_2 or CH_2 groups; these will not be discussed in the following sections, V, VI, and VII (which involve "normal" nido-structures without BH_2 or CH_2 groups), and are postponed for discussion in section XI on so-called abnormal nido-compounds, which follows discussions of arachno- and hypho-compounds (sections VIII, IX, and X), where BH_2 and CH_2 groups are commonplace. The endo-hydrogens of BH_2 groups are in seeming competition for electron density with bridge-hydrogens of very similar stability in the arachno- and hypho-compounds. The virtual equivalence of bridge and endo-hydrogens probably underlies the inherent fluxionality of many polyboranes.

Following the normal nido-compounds (sections VI and VII) and prior to the discussion of arachno- and hypho-compounds (sections IX and X), where the balance between bridging and endo-hydrogens assumes primary importance, section VIII will be interjected in which aliphatic hydrocarbons and arachno- and hypho-polyboranes are compared and the stabilities of bridge versus endo-hydrogens contrasted in an effort to rationalize the seemingly conflicting molecular
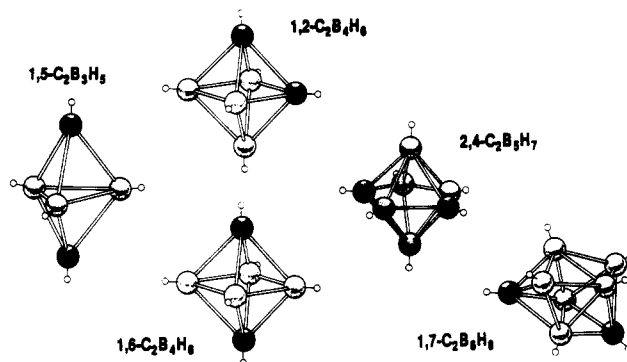
Figure 11. Smaller closo-carboranes.
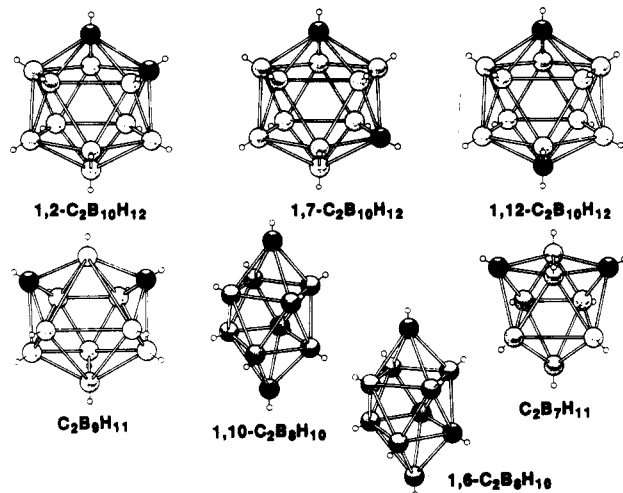
Figure 12. Larger closo-carboranes.

preferences for endo-hydrogens over bridge hydrogens in some cases and for bridge hydrogens over endo-hydrogens in closely related compounds.

Closo-compounds (section V) will be considered first.

V. Closo-Deltahedral Clusters

The most-spherical deltahedra[2,8,9] characteristic of the closo-polyborane dianions, $B_nH_n^{2-}$, -carborane anions, $CB_nH_{n+1}^-$, and -carboranes, $C_2B_nH_{n+2}$, are illustrated along the left hand side of Figure 6 and in section V.A. in Figure 14 (below). All of the polyborane dianions, $B_nH_n^{2-}$, wherein $n = 6-12$, have been isolated and structurally identified, and examples of all of the neutral closo-carboranes from five to eight vertices are illustrated in Figure 11. The larger carboranes with 9–12 vertices are illustrated in Figure 12. During the preparation of this review, Paetzold and Mennekes have reported a tetraalkyl derivative of the tetrahedral closo-B_4H_6 (not shown)[16b] which contains two opposing 3c2e bridge hydrogens!

The carbon placement rules immediately became apparent when the structures of the first carboranes, $1,5$-$C_2B_3H_5$, $1,2$-$C_2B_4H_6$, $1,6$-$C_2B_4H_6$, and $2,4$-$C_2B_5H_7$, were deduced from their ^{11}B NMR spectra[17] (Figure 11). The carbons were found in sites of lowest connectivity, when choices existed, and when alternative sites of identical connectivity were available, the carbons in the thermodynamically most stable isomers were found in nonadjacent locations. Later, these considerations allowed the easy prediction of the correct structures for
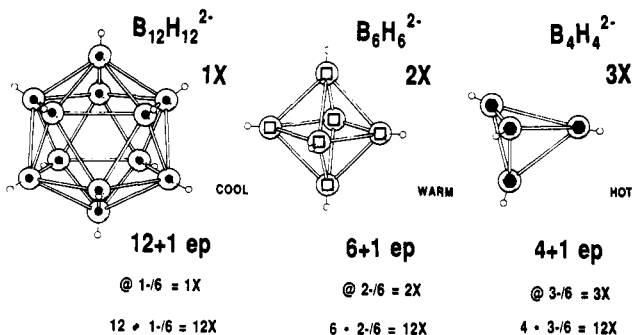
Figure 13. Icosahedral, octahedral, and tetrahedral charge distributions.

$1,7\text{-}C_2B_6H_8{}^{18}$ (Figure 11) and $2,3\text{-}C_2B_9H_{11}{}^{19}$ (Figure 12) in spite of ambiguous ^{11}B NMR spectra and foreshadowed the most stable structures for the other *closo*-carboranes and *closo*-carborane anions as well.

Lipscomb et al.[21] and Lonquet-Higgins and Roberts[20] predicted the existence of the icosahedral *closo*-$B_{12}H_{12}{}^{2-}$ and the octahedral $B_6H_6{}^{2-}$ dianions while groups led by Muetterties and Hawthorne isolated most of the *closo*-$B_nH_n{}^{2-}$ representatives.[22] Hawthorne's group also discovereed the intermediately sized *closo*-carboranes with seven, eight, and nine boron atoms[23] (Figure 12). Numerous space isomers have been found among the dicarba-*closo*-carboranes (Figure 11). Two or three groups of investigators, including (but not limited to) those of Bobinsky, Heying, Schroeder, Fein, Hillman, Grafstein, and Dvorak, discovered the three isomers of the most important *closo*-carborane, $C_2B_{10}H_{12}$, independently.[24] The writer was isolated from the laboratories where the *closo*-$C_2B_{10}H_{12}$ isomers were investigated as well as meetings where they were discussed and is aware that apparently there are still others whose work went unpublished.

A. Electron Distribution in the 5–14-Vertex *closo*-$B_nH_n{}^{2-}$ Clusters[2]

There are three candidate regular deltahedral polyborane dianions (Figure 13), the known icosahedral *closo*-$B_{12}H_{12}{}^{2-}$, the octahedral *closo*-$B_6H_6{}^{2-}$, and the tetrahedral [*closo*-$B_4H_4{}^{2-}$]. [*closo*-$B_4H_4{}^{2-}$] is not expected to be stable in contrast to "*capo*"-B_4Cl_4 and perhaps *nido*-C_4H_4 (tetrahedrane), both of which have tetrahedral structures. Each of the three symmetrical closo-deltahedra would have the 2– charge distributed equally among its equivalent vertices (BH groups). Each of the 12 equivalent, 5 k, BH vertices in $B_{12}H_{12}{}^{2-}$ would thus be assigned $^1/_6{}-$ negative charge, each of the six equivalent, 4 k, BH groups in the octahedral $B_6H_6{}^{2-}$ would be assigned $^2/_6{}-$ negative charge while each of the four, 3 k, vertices in the tetrahedral $B_4H_4{}^{2-}$ (hypothetical) would be associated with $^3/_6{}-$ negative charge (Figure 13). The following is elaborated in detail elsewhere[2] and is included here in abridged form.

All other less symmetrical deltahedra (Figure 14) incorporate mixtures of the same 3 k, 4 k, and 5 k vertices discussed above, and the same charges may be assigned to each BH vertex, that is, 3 k = $^3/_6{}-$, 4 k = $^2/_6{}-$, and 5 k = $^1/_6{}-$ in all cases, exactly as in the three symmetrical deltahedra. The total charge on each deltahedron always adds up to $^{12}/_6{}-$ or 2– no matter what the shape or size of the deltahedron or whether it is most spherical or least spherical.
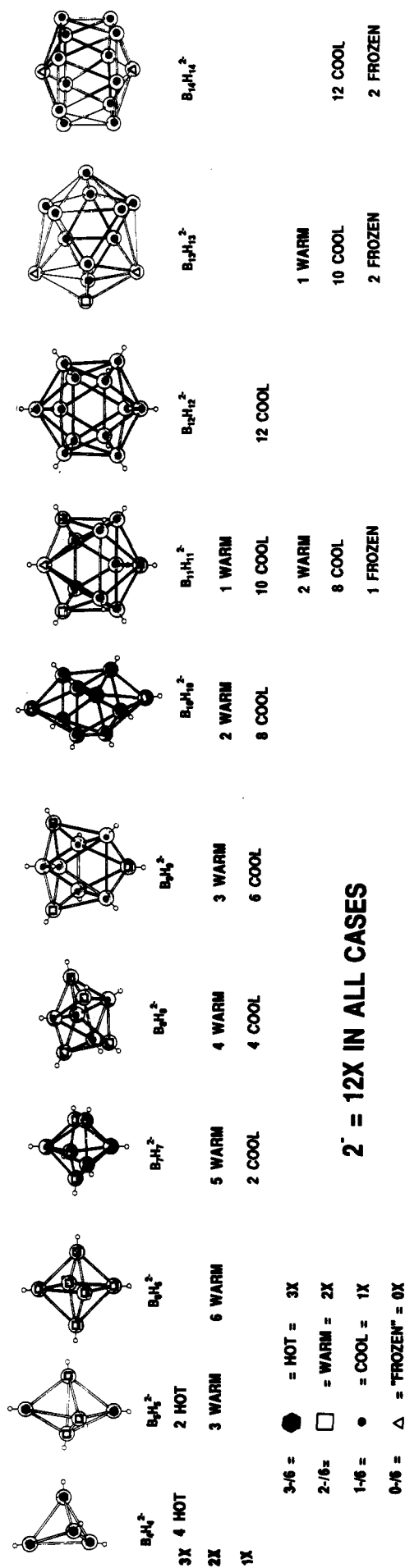

Figure 14. Most-spherical[2,8,9] closo-deltahedral charge distributions.

The connectivity of the various vertices are coded with a black hexagon representing the 3 k vertices (which we entitle "hot" to reflect the greatest negative charge, i.e., $^3/_6$–), an open square for the 4 k vertices ("warm", $^2/_6$–), and a solid dot in the 5 k vertices ("cool"; $^1/_6$–). An open triangle identifies 6 k vertices ("frozen"; $^0/_6$–).

In Figure 14 are illustrated all of the most spherical deltahedra, from the hypothetical $[B_4H_4{}^{2-}]$ to the undiscovered $[B_{14}H_{14}{}^{2-}]$ and the various vertices are labeled as hot, warm, cool, or frozen to indicate the amount of negative charge that simplistically would be associated with the various kinds of BH vertices in the various deltahedra. The total negative charge in all deltahedral species equals 2–.

These primitive electron density distribution codes (Figure 14) will be used in numerous examples throughout this review. The "excess" negative charge (over and above neutrality) is always 2– for the various $B_nH_n{}^{2-}$ closo-core-clusters but is 4–, 6–, and 8– for the nido-, arachno-, and hypho-polyborane core-clusters, $B_nH_n{}^{4-}$, $B_nH_n{}^{6-}$, and $B_nH_n{}^{8-}$, which are in turn derived from the parent nido-B_nH_{n+4}, arachno-B_nH_{n+6}, and hypho-B_nH_{n+8} classes, respectively.

In order to convert our primitive treatment of distributing the excess negative charge from closo-core-clusters (Figure 14) to nido-core-clusters, we deliberately focus on the connectivity, k, of the various kinds of BH vertices (which does not vary from closo to nido) rather than on the negative charge to be distributed as a function of k (which does vary from closo to nido). We can retrocalculate the crude charge distributions later.

Thus, the $^3/_6$–, $^2/_6$–, and $^1/_6$– negative charges (characteristic of 3 k, 4 k, and 5 k vertices in closo-$B_nH_n{}^{2-}$ compounds) are converted to $3X$, $2X$, and $1X$ negative charge, which preserves the relative values as a function of connectivity but allows X to vary as a function of whether the total negative charge is 2–, 4–, 6–, or 8–. As will be illustrated below, the total value of X (per deltahedral fragment) varies inversely with the individual value of X (per vertex) and also varies as a function of aperture size in the nido-deltahedral fragments. The total value of X becomes larger as the aperture becomes larger, but the individual value of X becomes smaller while the charge remains constant.

As a result of this manipulation, we assign $3X$, $2X$, $1X$, and $0X$ negative charges to the 3 k, 4 k, 5 k, and 6 k vertices, respectively, in all closo-deltahedra (2– total charge; see lower left hand corner of Figure 14) as well as in similarly connected vertices in the nido-deltahedral fragments (of 4– total charge), recognizing that the ultimate value of X (in actual negative charge) will vary from class to class, e.g. closo to nido, etc., and within each class as a function of aperture size, i.e., tetragonal (IV-gonal), pentagonal (V-gonal), and hexagonal (VI-gonal).

B. Electron Distribution in closo-Carboranes Extrapolated from Electron Distribution of $B_nH_n{}^{2-}$ Clusters

As an introductory example, consider the simple conversion of closo-$B_{12}H_{12}{}^{2-}$ (Figure 13) into 1,12-$C_2B_{10}H_{12}$ (Figure 12) by the hypothetical injection of two protons into two opposed ^{11}B atoms, producing the ^{12}C atoms. This simple "alchemical transmutation of

the elements" may be rationalized as follows: In Figure 13, the structure of $B_{12}H_{12}{}^{2-}$ was allocated $1X$ (or $^1/_6$–charge) to each 5 k, BH vertex. Next, we hypothetically inject two protons ($^6/_6$+ each) into opposed ^{11}B atoms, converting them into ^{12}C atoms. It would now seem that the two CH units (previously of $^1/_6$– charge) would become $^5/_6$+ charged as long as the skeletal-electron distribution remained distributed exactly as they were prior to the hypothetical injection of the two protons. This oversimplified situation, labeled a possible bond network, is a contrived convenience to rationalize where the carbons would tend to migrate in order to maximize charge smoothing in the most thermodynamically stable configurations when the carbons have choices between 3 k, 4 k, and 5 k locations (see below).

The possible bond network incorporates unrealistic charge distributions which would undergo subsequent adjustment due to the relative number of electrons donated and the electronegativities of the various atoms. It is recognized (of primary importance) that the carbon is a three-skeletal-electron donor (compared to boron which is a two-skeletal-electron donor) and that (of secondary importance) the electronegativity of the carbon is greater than the electronegativity of both boron and hydrogen and that these two characteristics of carbon would inductively attract the skeletal-electron distribution toward the carbons and away from the neighboring borons and hydrogens. Because of the greater number of electrons donated by carbon and the greater electronegativity of the carbon, the hydrogens connected to carbon by CH bonds become significantly more positively charged than the hydrogens bonded to boron by BH bonds.

In a second example, it would be expected that the carbons would concentrate in the 1- and 10-positions of the closo-10-vertex deltahedron (Figure 12) because of carbon–carbon repulsion and the greater electron density available in the 4 k vertices ($^2/_6$–) (Figure 14) as opposed to the 5 k vertices ($^1/_6$–). Indeed, on this basis, the structure and superior stability of closo-1,10-$C_2B_8H_{10}$ (Figure 12) was predicted[25a] and later confirmed.[25b]

VI. Nido-Deltahedral Fragment Considerations

A. Electron Distribution among Nido-Configurations

As illustrated in Figure 14, the "largest open face" of all nonaberrant closo-clusters is a triangle (III-gon). The total negative charge in the entire deltahedral closo-$B_nH_n{}^{2-}$ series (where the largest open faces are III-gons) is 2– (or $12X$), regardless of how varied the connectivity of the vertices in the various most spherical deltahedra (or other much less spherical deltahedra—not shown). As we remove connections from the closo-deltahedral structures to produce nido-deltahedral fragments, vertices of lower connectivity around sequentially larger open faces are produced.

Consider the $B_8H_8{}^{2-}$ dianion in Figure 15. As long as it remains a closo-deltahedral cluster, the total value of X for the entire cluster is necessarily $12X$ or 2– (X = 0.167–). The breaking or removal of one connection between two high-coordinated 5 k vertices converts two cool 5 k vertices ($1X$) into two warm 4 k vertices ($2X$). This also causes the formation of a nido-IV-gonal open
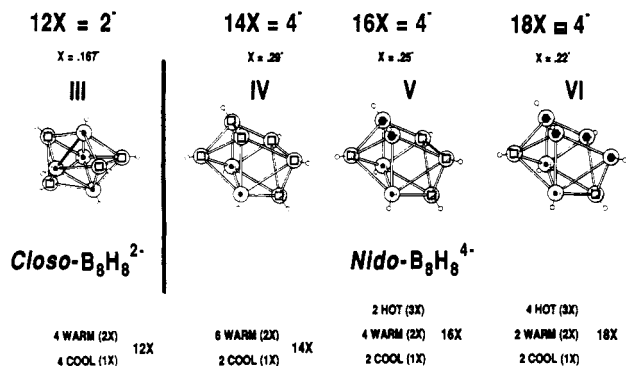
12X = 2⁻   14X = 4⁻   16X = 4⁻   18X = 4⁻

X = .167   X = .29⁻   X = .25⁻   X = .22⁻

III   IV   V   VI

Closo-B₈H₈²⁻   Nido-B₈H₈⁴⁻

2 HOT (3X)   4 HOT (3X)

4 WARM (2X)   6 WARM (2X)   4 WARM (2X)   2 WARM (2X)
          12X   14X   16X   18X
4 COOL (1X)   2 COOL (1X)   2 COOL (1X)   2 COOL (1X)

Figure 15. Conversion of closo-B₈H₈²⁻ into nido-B₈H₈⁴⁻ alternatives.

face from two previously III-gonal facets and the total value of X in the cluster to increase from $12X$ to $14X$. As this cluster is a nido-cluster, then the total charge is 4− and $X = {}^{4-}/_{14} = 0.29-$.

It follows (top of Figure 15) that repetition of the connection-removal procedure to produce open nido-faces with V-gonal open faces and VI-gonal open faces requires the total values of X to increase from $14X$ to $16X$ and $18X$ while the individual value of X in these nido-configurations decreases from 0.29− to 0.25− to 0.22−, respectively.

Since nido-core-clusters, $B_nH_n{}^{4-}$, derived from nido-B_nH_{n+4} compounds, have a 4− charge instead of the 2− charge characteristic of closo-deltahedral dianions $B_nH_n{}^{2-}$, the individual value of X increases by about 70% (0.167− to 0.286−) in going from closo-deltahedra (all III-gonal facets, $12X$ total) to nido-deltahedral configurations, which incorporate one IV-gonal open face per fragment ($14X$ total).

The quid pro quo is as follows: As connections are removed, the nido-open faces become larger (IV → V → VI) ($14X → 16X → 18X$) and lower connected (cool → warm → hot) vertices become more prevalent (5 k → 4 k → 3 k), but since the individual value of X declines simultaneously, the electron density values at identically connected vertices increase in the inverse order (VI → V → IV). In other words, 3 k vertices (hot) are more frequently (but not always) found neighboring VI-gonal open faces than about V-gonal open faces, but since $3X$ equals 0.75− for a 3 k vertex (rare) neighboring a V-gonal open face but only 0.67− for a 3 k vertex (abundant) neighboring a VI-gonal open face, the former is favored when ideal environments for one or two atoms are needed, and the latter is preferred when the optimal environments are needed for more than two atoms.

As long as the carborane skeleton is composed exclusively of carbons (three-skeletal-electron donors) and borons (two-skeletal-electron donors), the preferred nido-8-vertex fragment has the VI-gonal open face with four 3 k (0.67−) vertices, which comfortably accommodates up to four bridge hydrogens or up to four carbons. In contrast, when a sulfur (a four-electron donor) is present, the sulfur inductively attracts skeletal electrons, which makes the rest of the cage incrementally more electron deficient. This in turn promotes more connections and smaller apertures (section I.B. and Figure 1). The sulfur gains the added benefit of occupying a 3 k vertex of 0.75− charge characteristic of a V-gonal open face (Figure 6) rather than the 0.67−

charge characteristic of the four 3 k vertices about a VI-gonal open face.

In Figure 6, the larger scale structures identify the preferred structural configurations for the nido-species with boron–carbon skeletons incorporating 4 vertices (e.g., nido-C₄H₅⁺) to 12 vertices (e.g., the isomers of C₄B₈H₁₂). The 4- and 5-vertex nido-compounds are characterized by IV-gonal open faces, the 6-, 7-, 9-, and 11-vertex nido-compounds favor V-gonal open faces while the 8-, 10-, and 12-vertex nido-compounds adopt VI-gonal open faces (Figure 7).

B. Relative Bridge-Hydrogen Acidities

Within the nido-polyboranes, decaborane, $B_{10}H_{14}$, is more acidic than B_6H_{10}, which, in turn, is more acidic than B_5H_9. As explained by Parry and Edwards[25c] these three species are in essence core-clusters of $B_nH_n{}^{4-}$ plus four bridge hydrogens. It makes sense that the 4− spread over the nido-cluster $B_{10}H_{10}{}^{4-}$ would have less capacity to attract the four bridging hydrogens than would the smaller $B_5H_5{}^{4-}$ nido-cluster as the 4− is spread over half the number of BH units.

All three compounds (Figure 4) incorporate 66-bridge hydrogens.[8] The sixes represent the total coordination numbers of the two borons linked by the bridge hydrogen. *The bridge is counted as linked to each boron to get the proper coordination number.* In other words, B_5H_9 has four 66-bridge hydrogens as all four borons about the open face are 6-coordinate. The compound $B_{10}H_{14}$ also incorporates four 66-bridge hydrogens. B_6H_{10} has two 66- and two 65-bridge hydrogens about its base.

There is a need to differentiate between the *maximum* total coordination number of various atoms (where we count all other atoms within bonding distance of the atom under consideration) and the *minimum* simple connectivity, k, of deltahedral vertices (where we count only the limited number of vertices that connect to the vertex under consideration). The connectivity, k, values are most useful, before the fact, in estimating vertex charge distributions which in turn allow us to project where heteroatoms are most likely to migrate. In contrast the coordination numbers are most useful, after the fact, in projecting the thermal stabilities of various groups.

When atoms occupying differentially connected vertices are under consideration, e.g. 3 k, 4 k, and 5 k, we focus upon how many neighboring vertices are present. For example, a BH group occupying a vertex associated with five other neighboring vertices is designated as a 5 k vertex or a 5 k BH group; the exo-terminal hydrogen is ignored, as would be any bridge hydrogens if they were present. This allows us to designate, for example, an iron atom in a Fe(CO)₃ group that is associated with five neighboring vertices as a 5 k vertex or as a 5 k Fe atom. In this case the three exo-terminal CO groups are ignored and the 5 k BH and 5 k Fe(CO)₃ groups may almost be considered interchangeable, but their coordination numbers are quite different.

In contrast, when the focus is upon bridging hydrogens (associated with two borons) or endo hydrogens (associated with one boron), all of the borons and hydrogens in contact with the two borons or one boron are of interest and are counted in the bridge hydrogen identifying coordination numbers. In Figure 4, all four

66-bridge hydrogens in nido-B$_5$H$_9$ are located between two 3 k borons, as far as the skeletal vertices are considered; although each of the neighboring basal borons is 6-coordinate (three borons, two bridge hydrogens, and one terminal hydrogen) as far as the bridge hydrogen descriptions are concerned. In nido-B$_{10}$H$_{14}$ all four 66-bridge hydrogens are located between one 3 k boron and one 4 k boron, but the borons are 6-coordinate.

The term k applies only to the connectivity relationships of skeletal vertices to each other while the coordination numbers identifying bridge hydrogens refer to the total number of other atoms that are within bonding distance of their neighboring boron atoms.

Lower coordination numbers corrolate with the stability of the molecules with which they are associated; as an example molecules incorporating 66-bridge hydrogens are more stable than molecules incorporating 76-bridge hydrogens. For example, neutral nido-compounds are stable when they incorporate 66-bridge hydrogens but not stable when 76-bridge hydrogens are present. As an extension of this trend, arachno-polyboranes can accommodate the less stable 76-bridge hydrogens (and the almost as unstable 6'6-bridge hydrogens; see below). hypho-Polyboranes can even accommodate 77-bridge hydrogens (or the almost as undesirable 6'6'-bridge hydrogens). This pattern reflects the increasing capacity of the more hydrogen-rich polyboranes to attract and to retain increasingly more labile bridge hydrogens. For the present, it is enough to state that 76-bridge hydrogens are unacceptable among neutral nido-polyboranes at ambient conditions; although at very low temperatures, Shore has been able to produce B$_{11}$H$_{15}$[26] which probably incorporates two 76-bridge hydrogens.

C. Endo- and Bridge Hydrogens In Nido-Compounds

Within the nido-compounds, almost all of the skeletal hydrogens (inner sphere hydrogens) are found as bridge hydrogens rather than as endo-hydrogens with the exceptions of nido-4-vertex compounds, one nido-7-vertex compound,[27] Shore's[26] nido-B$_{11}$H$_{14}$⁻ (which involves an endo-hydrogen), and nido-B$_{11}$H$_{15}$, which must involve endo-hydrogens. Sneddon[28] has also found one aberrant nido-10-vertex compound, C$_3$B$_7$H$_{11}$, where apparently one endo hydrogen is forced to occupy an endo-hydrogen location on carbon as the placement of the three carbons eliminates all more favorable locations for a bridge hydrogen. nido-Diborane, B$_2$H$_6$, the "misfit of the boron hydrides" (Figure 1) also incorporates endo-hydrogens.

Discussion of nido-compounds which incorporate BH$_2$ groups will be postponed until section XI following the discussions on the arachno- and hypho-polyboranes (sections IX and X) where BH$_2$ groups are prevalent.

VII. Nido-Compounds (without BH$_2$ Groups)

nido-[B$_3$H$_7$][29] and nido-[B$_4$H$_8$] have never been isolated but have been postulated as intermediates. The anion of the latter, nido-B$_4$H$_7$⁻, has been tentatively reported[30] and the isoelectronic and probably isostructural analogue C$_4$H$_5$⁺, has been reported by Olah[31] and structurally identified with certainty.[31,32] It has our predicted[9] nido-4-vertex configuration for electron-de-

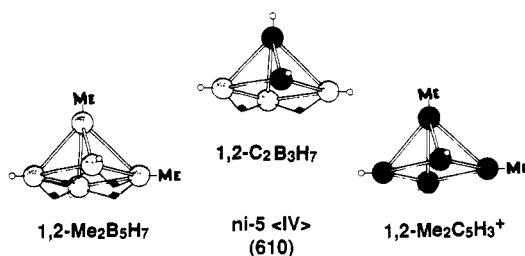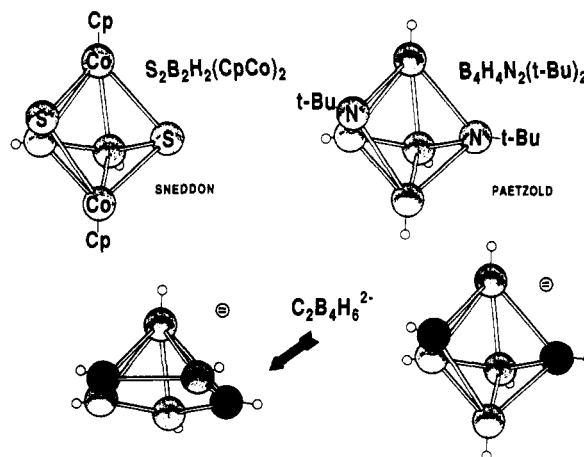
Figure 16. Nido-5-vertex compounds (Stx = 610).

Figure 17. Nido-6-vertex compounds (Stx = 620).

ficient species (Figure 6), but as it contains a CH$_2$ group, it will be discussed in section XI along with other nido-compounds which incorporate BH$_2$ or CH$_2$ groups.

A. Nido-5-Vertex Family

nido-1,2-(CH$_3$)$_2$B$_5$H$_7$,[33] a related carborane, 1,2-C$_2$B$_3$H$_7$,[34] and the (1,2-CH$_3$)$_2$C$_5$H$_3$⁺ carbocation[9,35] are illustrated in Figure 16. One carbon in the carborane assumes the less desirable higher coordinate 4 k, 1-position to allow the bridge hydrogens to have access to neighboring borons about the open face. We are confident that nido-1,2-(CH$_3$)$_2$C$_5$H$_3$⁺ is the most stable carbocation isomer as one of the methyl groups stabilizes the most electron deficient, higher 5-coordinated apex carbon rather than the lower 4-coordinated basal carbons. In contrast, Onak's nido-1,2-(CH$_3$)$_2$B$_5$H$_7$ rearranges upon heating into the more stable 2,3- and 2,4-isomers in order that the methyl groups contribute to the more electron deficient, higher (6-coordinated) base borons rather than the lower (5-coordinated) apex boron. In both the all-boron and all-carbon skeletons the apex atom is in the higher 4 k site while the basal atoms are in the lower 3 k sites. The situations are reversed, however, when the coordination numbers are compared, because the bridge hydrogens make the basal borons more highly coordinated than the apex boron.

B. Nido-6-Vertex Family

Although Figure 3 illustrates many isoelectronic and isostructural ni-6⟨V⟩ compounds, there are other isoelectronic compounds that have alternative ni-6⟨IV⟩ structures with smaller open faces due to the incorporation of two four-skeletal-electron donors such as RN[36] or :S,[37] etc. (Figure 17).

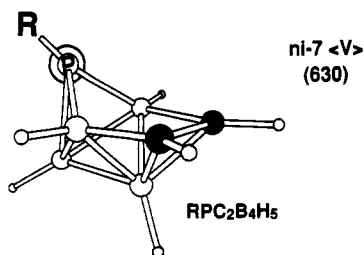The four-skeletal-electron-donor atoms inductively attract electron density away from the rest of the

Figure 18. Nido-7-vertex compound (Stx = 630).

cluster. The resulting incrementally greater electron deficiency promotes increased connectivity, which in turn results in smaller open faces. The four-skeletal-electron donors (in this case) gain access to 3 k vertices of greater electron density also. The carbons (only three-skeletal-electron donors) in 2,4-$C_2B_4H_6{}^{2-}$ are unable to cause greater connectivity.[38] Apparently one or two four-electron-donor atoms must be present to cause increased connectivity.

C. Nido-7-Vertex Family

Hosmane et al.[39] have reported the first ni-7⟨V⟩ compound without an endo-hydrogen or other endo-group (Figure 18). Their compound incorporates one four-skeletal-electron donor (RP) and two three-skeletal-electron donors (RC). The ni-7⟨V⟩ configuration provides three electron rich environments (at 0.75−) for these three atoms. We suggest that if the two RC groups were replaced by two isoelectronic HB⁻ moieties, then the alternative ni-7⟨IV⟩ structure (Figure 6), which would provide one 0.86− vertex for the lone RP group, would be the preferred configuration.

D. Nido-8-Vertex Family

Two compounds with heretofore debatable structures have recently been found to have the same ni-8⟨VI⟩ configuration as several other related species. The compounds, B_8H_{12},[40] $R_4C_4B_4H_4$,[41] and R_4C_4-(CpCo)B_3H_3,[42] had long been known to have ni-8⟨VI⟩ structures (Figure 19). Our recent ab initio/IGLO/NMR calculations[43] confirmed the ni-8⟨VI⟩ structure for nido-$C_2B_6H_{10}$[44] (and, by inference, the structure of Sneddon's $B_8H_{10}L$[45]); L = NEt₃.

The alternative ni-8⟨V⟩ structure with one more connection and a smaller open face is favored as a result of incrementally greater electron deficiency when one four-skeletal-electron donor, sulfur, is present as in

nido-S(CpCo)₂B_5H_7. The sulfur also gains access to a 3 k vertex of 0.75− charge rather than 0.67− charge characteristic of 3 k vertices in the ni-8⟨VI⟩ configuration.

In applying the ab initio/IGLO/NMR technique, the various competitive structures are subjected to ab initio structural optimization following which IGLO calculations are used to predict the sets of ¹¹B and ¹³C chemical shift values to be expected of each ab initio optimized structure. The predicted sets of NMR values are compared to the experimentally determined NMR values, and a very close match is usually found for one and only one structure.

Kutzelnigg is the pioneer–discoverer of the IGLO technique,[47] Schindler and Kutzelnigg applied it to nonclassical carbocations,[48] and Schleyer extended it to other carbocations[49] and to the refinement of other arachno-polyborane structures,[50] notably B_5H_{11} and B_6H_{12}.

E. Nido-9-Vertex Family

It is improbable that nido-[B_9H_{13}] can be made at ambient conditions as it would incorporate either one 77-bridge hydrogen and two 76-bridge hydrogens (Stx = 650) or an equally unfavorable endo-hydrogen (Stx = 461). The removal of only one proton to produce $B_9H_{12}{}^-$ (650) eliminates the 77-bridge hydrogen and both 76-bridge hydrogens simultaneously. nido-$B_9H_{12}{}^-$ in the ni-9⟨V⟩ configuration[51] is quite stable (Figure 20) as predicted.[8]

Carboranes are also stable in the ni-9⟨V⟩ configuration, but when two sulfurs (four-skeletal-electron donors) and two CpCo groups are present,[52] the ni-9⟨IV⟩ configuration is chosen. In this case the two sulfurs cause the incrementally greater electron deficiency, which causes the increased connectivity and the resulting smaller aperture, but in this case, the two sulfurs, in gaining access to two 0.57− vertices rather than to one 0.75− and one 0.50− vertex, lose in net electron density.

Surprisingly to us, two CpNi and two carbons (all four groups are three-electron donors) also promote the ni-9⟨IV⟩ configuration. Since four carbons probably would not cause the selection of the ni-9⟨IV⟩ configuration, the two CpNi groups are probably responsible. Perhaps CpNi groups are more electronegative than comparable carbon groups and thus promote just enough additional incremental electron deficiency to favor the more compact ni-9⟨IV⟩ configuration.
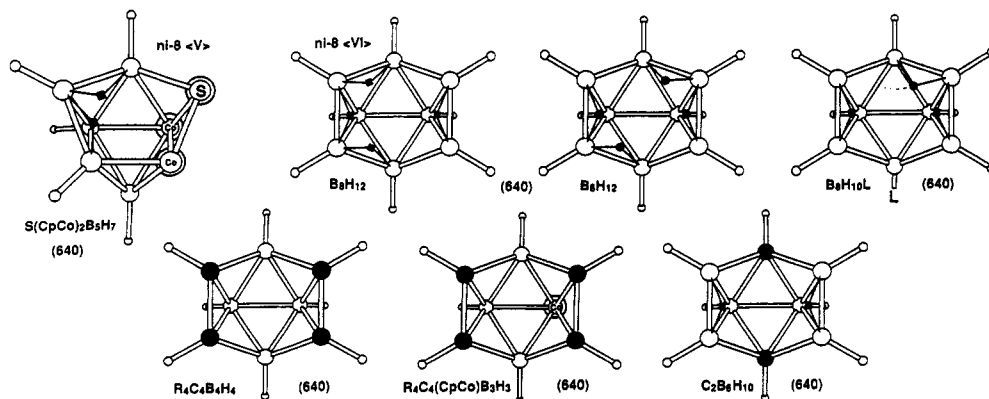

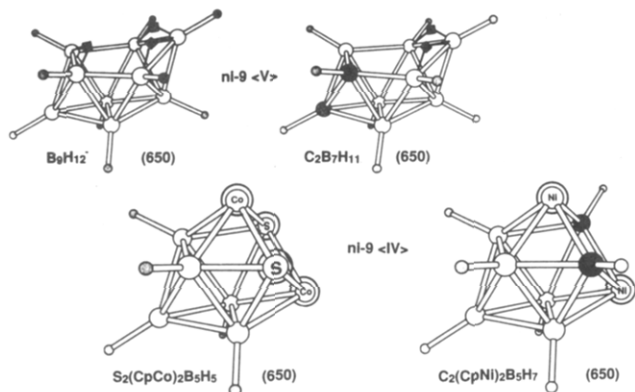**Figure 19.** Nido-8-vertex compounds (Stx = 640).

Figure 20. Nido-9-vertex compounds (Stx = 650).

Figure 21. Nido-10-vertex compounds (Stx = 660).

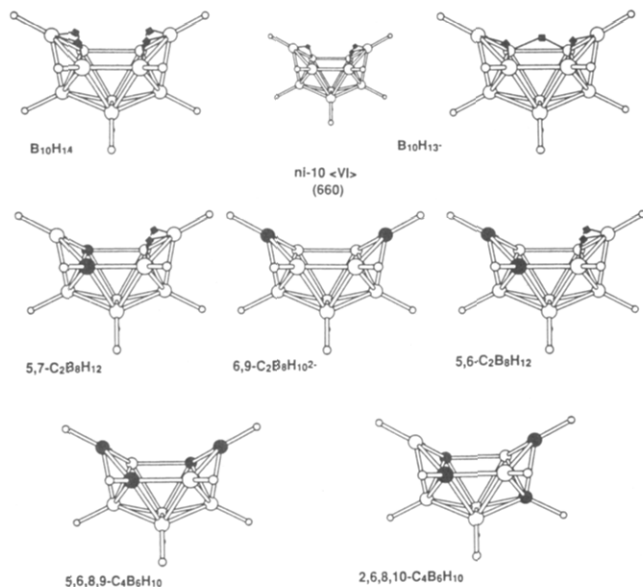**Figure 22.** Nido-11-vertex compounds (Stx = 670).

F. Nido-10-Vertex Family

nido-Decaborane, $B_{10}H_{14}$ (Figure 21), is the most stable *nido*-polyborane and has the ni-10⟨VI⟩ structure (Stx = 660), as do a myriad of related carboranes and carborane anions. The anion $B_{10}H_{13}^-$ has a different 660 structure in the crystal (smaller illustration) than in solution (larger illustration) to accommodate crystal-packing forces in the former and bridge-hydrogen preferences in the latter.[53,54] Skeletal hydrogen stability analysis (section VIII, below) favors the structure in solution.

When bridge hydrogens are absent, the carbons occupy the lowest coordinated sites;[55] see *nido*-6,9-$C_2B_8H_{10}^{2-}$; but when two protons are added to 6,9-$C_2B_8H_{10}^{2-}$, the product rearranges[56] into *nido*-5,6-$C_2B_8H_{12}$ (details elsewhere[2]). When four carbons and no bridge hydrogens are present, e.g., Hermanek's[57] 5,6,8,9- and Koster's[58] 2,6,8,10-$C_4B_6H_{10}$ isomers, the ni-10⟨VI⟩ configurations are adopted, but in the latter a strong distortion toward the assumption of a ni-10⟨V⟩ configuration (not illustrated in Figure 21) is noted in the actual crystal structure.[2] We predict[2] that $SB_9H_{10}^-$ (with one bridge hydrogen) and $SB_9H_9^{2-}$ (with no bridge hydrogens) can be produced and that the ni-10⟨V⟩ configuration will probably be observed in the former
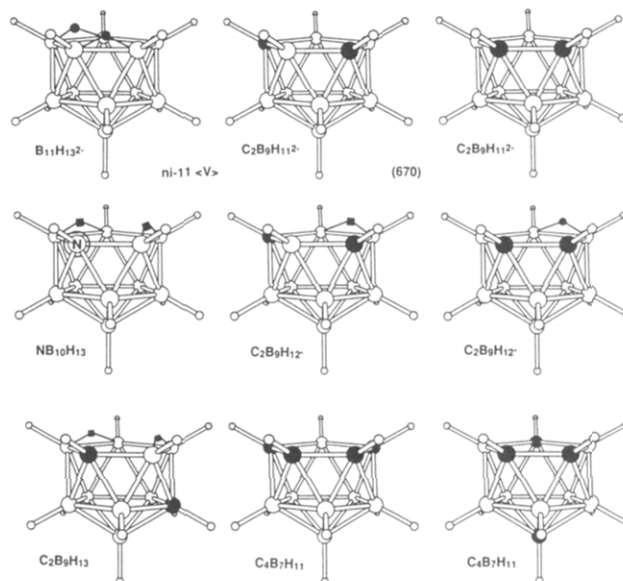
and certainly in the latter due to the greater incremental electron deficiency induced by the sulfur.

Alternatively, when a relatively electropositive Ru-(C_6Me_6) group (a two-skeletal-electron donor) substitutes for a boron in the 1-position, an unusual ni-10-⟨VII⟩ configuration is assumed.[59]

G. Nido-11-Vertex Family

nido-$B_{11}H_{13}^{2-}$[60] (Figure 22) is the prototype for nido (Stx = 670) compounds as it incorporates 66-bridge hydrogens in anionic environments as do both isomers of $C_2B_9H_{12}^-$ and $CB_{10}H_{13}^-$. All have ni-11⟨V⟩ configurations. The neutralization of these favorable anionic environments by the addition of protons necessarily creates congestion, i.e., the production of 76-bridge hydrogens and unstable endo-hydrogens. Thus, the discussion of *nido*-$B_{11}H_{14}^-$ and *nido*-$B_{11}H_{15}$ as well as isomers of $C_2B_9H_{13}$ will be postponed and covered in section XI.

In a few of the nido-11-vertex species, carbons assume 5 k cage positions rather than 4 k edge positions in order to accommodate bridge hydrogens about the open face (see also 1,2-$C_2B_3H_7$ in Figure 16).

Several isomers of $C_4B_7H_{11}$ have also been observed;[2,61,62] all have ni-11⟨V⟩ configurations. The presence of four-skeletal-electron donors cannot cause nido-11-vertex compounds to adopt deltahedral fragment structures with IV-gonal apertures, and thus, RN, :S, and RP groups are found about the open face of the ni-11⟨V⟩ configuration.

It was not anticipated that any ni-11⟨IV⟩ configuration would be observed as it is not a fragment of a regular icosahedron but Greenwood et al. have found one such aberrant compound[63] when certain transition element groups were present.

H. Nido-12-Vertex Family

Grimes[12,64] discovered several C-alkyl derivatives of *nido*-$C_4B_8H_8$ and determined their ni-12⟨VI⟩ structures. An alternative isoelectronic (but not isostructural) configuration incorporates a 6 k vertex on a cage position;[2] it is designated as having a ni-12⟨VI*⟩ structure
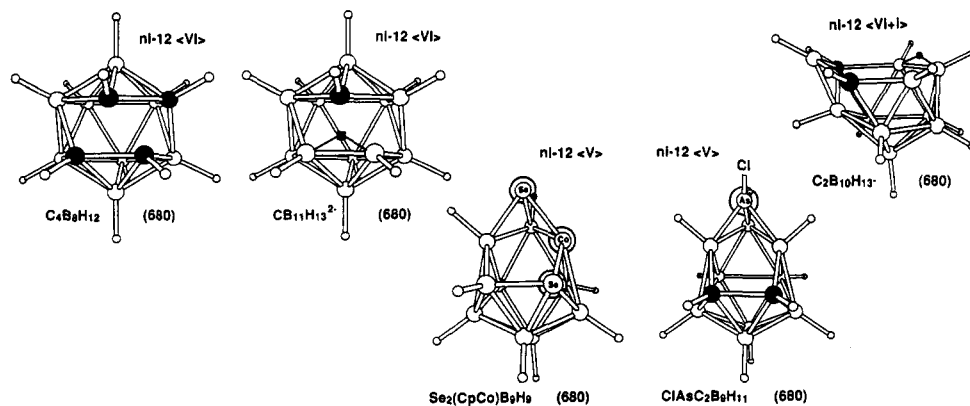
Figure 23. Nido-12-vertex compounds (Stx = 680).

(not shown); the asterisk indicates the presence of a 6 k vertex in a cage position (Figure 23).

When only borons and carbons are present as skeletal atoms, the ni-12⟨VI⟩ configuration is preferred.[11] However, when a sufficiently electropositive transition element atom is present, isomers containing both ⟨VI⟩ and ⟨VI*⟩ open faces (Figure 6) may be found.[2,12] Upon heating, certain ni-12⟨VI⟩ isomers will rearrange[12] into more stable ni-12⟨VI*⟩ configurations, if and only if an appropriate transition element atom is present to occupy the 6 k site. An unstable C-alkyl derivative of nido-$C_2B_{10}H_{13}^-$ has a VI-gonal open face, but as no transition element atom is present, one connection between carbon and what would otherwise be a 6 k boron is absent, ⟨i⟩, in order that no 6 k vertices persist in the boron–carbon skeleton;[65] we identify this aberrant structure as a ni-12⟨VI+i⟩ configuration (Figures 6 and 23).

When one or two four-skeletal-electron-donor heteroatoms are present, incremental electron deficiency is increased, an additional connection results, and the ni-12⟨V⟩ configuration is observed; AsCl,[66] :Se,[67] etc.

Grimes' compound, $R_4C_4B_8H_8$,[2,64] can assume both the ni-12⟨VI⟩ configuration (shown) and an alternative ni-12⟨IV+IV⟩ configuration. This latter configuration may also be assigned an arachno-configuration as well, and our preference is to analyze it as if it were a 12-vertex arachno-compound; see section IX.K, Figure 40, e.g., ara-12⟨VI⟩ (Stx = 582).

VIII. Preamble to the Discussion of Arachno- and Hypho-Compounds: Hydrocarbon versus Polyborane Structures

When the entire range of polyboranes are compared with similarly sized aliphatic hydrocarbons, a number of generalities become apparent.

A. Aliphatic Hydrocarbon Macro- and Microconfigurations

There are hundreds of aliphatic hydrocarbon space isomers incorporating 2–12 carbons when double bonds, triple bonds, and cyclic moieties are included (and wherein the carbons are always associated with at least one terminal hydrogen). The various chains and rings, etc., in these electron-precise clusters give rise to an *enormous* number of stable molecular arrangements in space for the carbons (macroconfigurations) which far exceed the space available for their illustration. On the
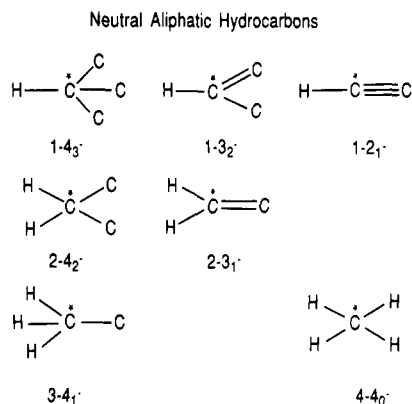

Figure 24. Seven oversimplified aliphatic hydrocarbon microconfigurations (contrived in order to expedite subsequent comparisons with polyborane microconfigurations).

Figure 25. Comparisons of aliphatic hydrocarbons and polyboranes.

other hand, the small architectural units (microconfigurations) used to "assemble" these innumerable macroconfigurations of neutral aliphatic hydrocarbons number only seven (Figure 24).

Our interest is in focusing on, and differentiating between, the different types of terminal hydrogens in the aliphatic hydrocarbons for subsequent comparison with the kinds of skeletal bridge and endo-hydrogens in the polyboranes. We do this by comparing the coordination situations of the carbons (C*) to which the terminal hydrogens are attached.

The number identifying each contrived aliphatic hydrocarbon microconfiguration is hyphenated and is followed by a subscript (Figure 24). The number before the hyphen identifies how many terminal hydrogens (1–4) are on the specific carbon under consideration (C*); the number following the hyphen identifies the total number of atoms coordinated to that carbon (C*). The following subscript identifies how many of that

Figure 26. Original 55- to 6'6'-bridge hydrogen evaluations.

total number were carbons; i.e., the subscript equals the total coordination number minus the number of hydrogens to which C* is coordinated.

In summary then, a minimum number of microconfigurations (Figure 25) can be put together in multifarious ways to produce a gigantic number of molecular structures (macroconfigurations) involving 2–12 carbons.

This situation is reversed in the polyboranes containing 2–12 borons. It will be shown that a quite limited number of boron-skeleton (Figure 6) macroconfigurations (varying only slightly in the disposition of their bridge and endo-hydrogens) are produced from a veritable hoard of microconfigurations.

B. Polyborane: Macro- and Microconfigurations

For well over 2 decades,[9] it has been recognized that all (or almost all) nido- and arachno-polyboranes (and carboranes) could be related to fragments derived from sequential removal of vertices and connections from that series of most spherical deltahedra characteristic of the closo-carboranes, $C_{0 \text{ to } 2}B_nH_{n+2}$ and $B_nH_n^{2-}$ (left hand column of Figure 6).

A comparison of Figures 3 and 6 foreshadows the generality that there are only a few macroconfigurations among the polyboranes despite the innumerable variations in the multitude of microconfigurations involving bridge or endo-hydrogens.

The skeletal bridge and endo-terminal hydrogens (inner sphere hydrogens) are attached to the boron skeleton by skeletal electrons while the exo-terminal hydrogens (outer sphere exo-terminal hydrogens) are not. To minimize confusion when both bridge and endo-hydrogens are under discussion, we will refer to them as skeletal hydrogens as illustrated.

skeletal hydrogens = { bridge hydrogens / endo-hydrogens / exo-hydrogens } = terminal hydrogens

We recognize that the difference between endo- and exo-hydrogens becomes moot when less than four skeletal borons and carbons are present as in nido-B_2H_6 and arachno-$B_3H_8^-$. The various types of bridge hydrogens are listed in Figure 26.

In 1976,[8] we differentiated between the types and kinds of bridge hydrogens (H**) by identifying the coordination numbers of the two borons (B*s) between which the bridge hydrogen is located (counting the bridge hydrogen in the coordination number count). It was found (empirically) that greater stability (less lability) was associated with smaller coordination numbers (e.g. 55 > 65 > 66 > 76 > 77); this will be considered to be the primary effect. It was also observed that bridge hydrogens between two borons of given coordination numbers were less stable between BH_2 groups than if they were between BH groups. Coordination
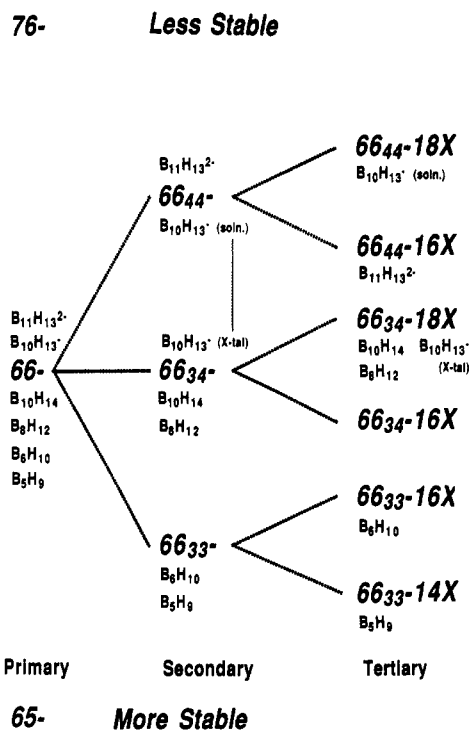

Figure 27. Primary, secondary, and tertiary bridge-hydrogen stability differences.

numbers labeling the borons in BH_2 groups were identified with primes (e.g. 5'5' > 5'6' > 6'6', etc.).

Concentrating on those factors that we thought engendered instability, and lacking additional insight at the time, we assumed that a 6'6'-bridge hydrogen (a bridge hydrogen between two 6-coordinate BH_2 groups) was almost as unstable as a 77-bridge hydrogen (a bridge hydrogen between two 7-coordinate BH groups). This led to Figure 26.

Recently, we have empirically correlated a secondary effect: bridge-hydrogen stability is also influenced by the specific identity of the atoms (other borons and other hydrogens) that make up the coordination numbers of the two borons (B*s) neighboring the bridge hydrogen (H**). The more borons in the coordination counts of the borons (B*s), the less the stability (Figure 27).

Accordingly, following the numbers identifying the total coordination numbers of the borons (B*s) neighboring the bridge hydrogens, subscripts have been added which identify the numbers of other borons attached to the neighboring borons (B*s) (secondary effect). A 66_{33}-bridge hydrogen (as is found in B_5H_9) indicates a bridge hydrogen (Figure 4) that is between two 6-coordinate borons (B*s) of which three of the 6-coordinated atoms are other borons in each case (Figure 27). A 66_{34}-bridge hydrogen (as is found in $B_{10}H_{14}$ in Figure 4) is slightly less stable and indicates a bridge hydrogen between two 6-coordinate borons, one of which is coordinated to three other borons while the second boron is coordinated to four other borons. Note that the 33 and 34 coincidentally coinside with the skeletal connectivity values (k) of the two borons neighboring the bridge hydrogens.

Among nido-compounds, it was noted that differences in bridge-hydrogen stability are also linked to aperture size or departure from a completed deltahedron; smaller apertures favor greater electron density and greater
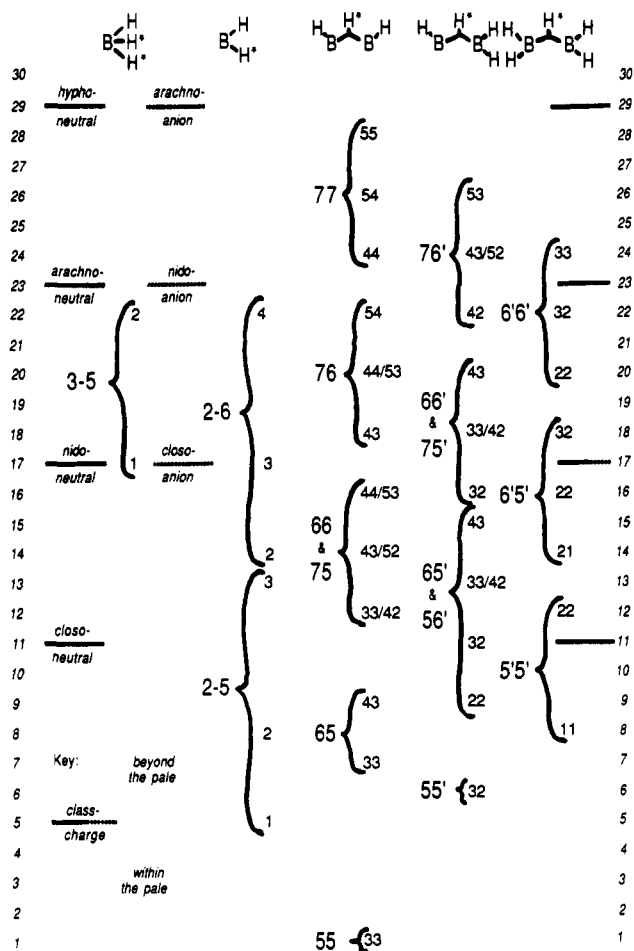
Figure 28. Microconfigurations of hydrogens and borons in the *closo*-, *nido*-, *arachno*-, and *hypho*-polyboranes (for comparison with "contrived" Figure 24.

bridge-hydrogen stability if coordination numbers remain constant. This is a tertiary effect.

The smaller apertures vary directly with the smaller total values of X as illustrated in Figure 27 and have been used previously in relating the increasing acidity[2] in the series *nido*-B_5H_9 < B_6H_{10} < B_8H_{12} < $B_{10}H_{14}$ (section VI.B. and Figure 26). The variations occasioned by the primary and secondary differences in microconfigurations are amplified and illustrated in Figure 28; tertiary effects are ignored for the present.

Figure 28 is speculative, is derived empirically, and reflects, at best, a "blurred vision or a first draft" of the factors influencing the relative stabilities of various microconfigurations which, when added together, seemingly parallel the stability or the lack of stability of the resulting macroconfigurations (caveat emptor).

Those microconfigurations illustrated toward the bottom of Figure 28 are associated with stability while those toward the top are associated with instability. The less stable microconfigurations (closer to the top of Figure 28) are empirically found to be increasingly more prevalent in the order closo < nido < arachno < hypho, which apparently reflects the increasing electron density availability to attract skeletal hydrogens as the skeletal electron count increases, i.e., $2n + 2 < 2n + 4$ < $2n + 6 < 2n + 8$, even though a proton is also added along with the addition of each electron. The less stable moieties (top of Figure 28) are understandably much more stable when they are incorporated into anions rather than neutral species, again reflecting the desirability of greater electron density in attracting skeletal hydrogens.

Figure 28 is based on the coalescence of two empirical patterns. Firstly, there seem to be many pairs or groups of very closely related *arachno*-polyborane structures that differ dramatically in how their skeletal hydrogens are distributed between bridge or endo-hydrogens.

Within all polyboranes, the total skeletal hydrogens (both bridge and endo) are those in excess of the number of exo-hydrogens in BH units. At one extreme are a few examples of the homogeneous nido-compounds, $B_5H_8^-$, $B_{10}H_{14}$, and $B_6H_{11}^+$, which incorporate three, four, and five skeletal hydrogens and have Stx identification numbers of 610, 660, and 620, respectively. As the x in Stx number is 0 in each case, there are no endo-hydrogens, and thus, all of the skeletal hydrogens in these three homogeneous nido-structures, as well as in most other nido-compounds, are bridge hydrogens.

In contrast, the distribution of the skeletal hydrogens between bridge and endo-hydrogens in the heterogeneous arachno-structures, as reflected by their Stx numbers, varies enormously, e.g., B_4H_{10} (502) vs $B_4H_9^-$ (313), and $B_9H_{13}^{2-}$ (363)[68] vs B_9H_{15} (930).[69] *arachno*-B_4H_{10} has two endo-hydrogens out of six skeletal hydrogens (33%) while its anion, $B_4H_9^-$, has three out of five (60%). Compound B_9H_{15} has six bridge-hydrogens out of six skeletal hydrogens (0%) while its dianion $B_9H_{13}^{2-}$ [68] has three endo-hydrogens and one bridge hydrogen (75%). Why would this be? Could the endo:bridge hydrogen ratio within the *arachno*-polyboranes be random? Are crystal-packing forces dominant? On the other hand, the ^{11}B NMR spectra of most arachno-compounds suggest that usually (but certainly not always) the same structure is detected in solution as in the crystal.

One explanation might be that bridge hydrogens (spanning two borons) and endo-hydrogens (spanning one boron?) lie on a continuum and are almost equivalent as far as their influence on overall molecular stability is concerned. Lacking a better alternative at this time, we offer Figure 28 as our primitive, empirical, best effort to compare the almost equivalent bridge and endo-hydrogens as a function of the stability or lack of stability imparted to given molecular structures by their presence.

A second pattern emerges when we consider that the skeletal hydrogens (both endo and bridge) are in competition for skeletal electrons and that skeletal hydrogens on borons (of otherwise identical coordination numbers) might be more stable or less stable as a function of the actual identity of the atoms (either borons or hydrogens) to which those coordination numbers apply (see secondary effect in Figure 27).

Extrapolating the primary and secondary effects from Figure 27 to Figure 28 highlights the effects of both the coordination number (of primary importance) and the atomic composition of those coordination numbers (of secondary importance). Endo- and bridge hydrogens (H**) are associated with either one (B*) or two (B*B*) borons which are in turn coordinated with other borons (B) and hydrogens (H) in varying numbers and ratios.

Thus, 76-bridge hydrogens are much less stable than 66-bridge hydrogens (primary effect). In a similar fashion, however, 66_{34}-bridge hydrogens are somewhat

less stable than 66_{33}-bridge hydrogens (secondary effect, Figure 27).

Endo-hydrogens identified with the label $2\text{-}6_3$ indicate B^*H_2 groups (the 2 counts the terminal hydrogens) in which the B^* is coordinated to six other atoms of which three are borons. In a fashion, similar to the way we evaluate bridge hydrogens, $2\text{-}6_3$-endo-hydrogens are more stable than $2\text{-}6_4$-endo-hydrogens. In the latter case, the boron of the BH_2 group is coordinated to four other borons. One is tempted to consider the possibility that perhaps greater electron density (related to increased stability) can more easily be preempted from neighboring hydrogens than from neighboring borons.

This runs counter to the long-accepted relative electronegativities of boron (2.0) and hydrogen (2.2), but Benson and Luo have recently (1989) recalculated[70] the electronegativity of hydrogen to be 1.61, which reverses the relationship of hydrogen to boron (2.0) and suggests that hydrogen-rich environments might indeed be more conducive to donating higher electron densities to neighboring atoms than boron-rich environments.

The vertical stability estimations of Figure 28 have been reverse-calculated by emperical comparisons of all known *arachno*-polyborane structures. Differences in degree between the stabilities of vertically adjacent sets of bridge hydrogens, e.g. 65, 66, 76, etc., have been assumed to differ in a monotonic fashion where they must be nonlinear to some degree; major refinements are needed.

That the structural components exhibited by many compounds fit the patterns derived from those exact same compounds is not surprising (circular reasoning), but the fact that patterns emerge at all debunks thoughts that the choices are random or chaotic in most cases and supports the supposition that only a few structures are different in the crystal (X-ray) due to crystal packing forces as compared to their less encumbered structures when in solution (NMR).

Figure 28 may be used in the following manner: First, when comparing two or more competing structures, identify the allowable range of microconfigurations that are acceptable, i.e., those that are within and/or below the pale (stability limit) for the specific class of neutral compounds, i.e., hypho- > arachno- > nido- > closo-species (upper limits are identified along the left hand margin of Figure 28).

Second, compensate for the presence of negative or positive charge; i.e., extend the acceptable stability range upward for anions, e.g., arachno-monoanions $\cong$ hypho-neutrals, and two classes up for dianions, e.g. nido-dianions $\cong$ hypho-neutrals, etc. (see Figure 28).

Third, for each skeletal-hydrogen microconfiguration within competing structures, identify the vertical locations for all skeletal hydrogens (both bridge and endo-hydrogens) in Figure 28.

Fourth, reject those structural alternatives which incorporate any microconfigurations whose vertical location is beyond and/or above the pale (stability range) for the species under consideration (Figure 28).

Fifth, consider rejecting structures involving any microconfigurations on or near the pale.

Sixth, consider most favorably those structures having features furthest from the borderline of instability and those structures where all skeletal hydrogens are grouped closest to each other in terms of stability, thus
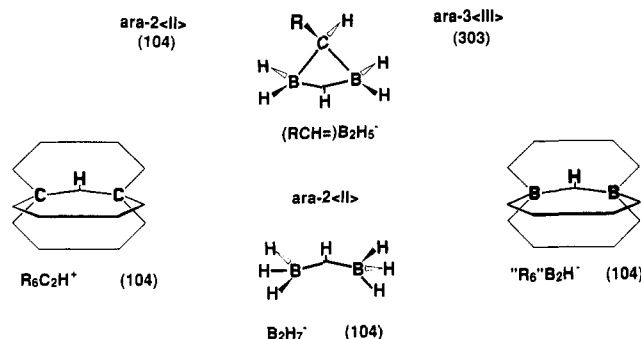

Figure 29. Arachno-2-vertex family.

maximizing charge smoothing. An unimpressed referee fittingly referred to the ephemeral relationships in Figure 28 as the Pale Scale.

In Figure 28, the endo-hydrogens on boron are treated in a similar fashion, as were the hydrogens on carbon in Figure 24. The hyphenated number $2\text{-}6_4$ identifies (from left to right) a central boron (B^*) to which is attached two terminal hydrogens (the 2) one of which is the endo hydrogen (H^{**}) whose relative stability is under consideration.

H^{**} = a $2\text{-}6_4$ endo hydrogen H^{**} = a $2\text{-}6_3$ endo hydrogen
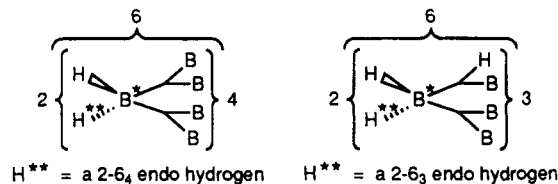
The central boron's (B^*) has a total coordination number of six (6) of which four (6_4) of the six neighboring atoms are four other borons (B). In a similar vein, $2\text{-}6_3$ identifies a BH_2 group where the central boron (B^*) is attached to six other atoms of which three are borons.

The bridge hydrogens (H^{**}) are represented by a nonhyphenated pair of numbers reflecting the total coordination numbers of the two boron atoms (B^*) between which the bridging hydrogen (H^{**}) is located. A pair of subscript numbers follow which identifies how many of the two total coordination numbers reflect coordination to "other" borons.

IX. Arachno-Compounds

Almost all closo-structures are comprised of one type of architectural unit, i.e., BH and CH groups. Many (or most) nido-structures incorporate a second feature, i.e., bridge hydrogens (BHB groups) in addition to BH and CH groups. Arachno-structures usually incorporate a third feature, i.e., endo-hydrogens in CH_2 or BH_2 groups in addition to BHB, CH, and BH units (Figure 10). There are a few nido-compounds that also incorporate endo-hydrogens; they will be addressed in section XI.

A. Arachno-2-Vertex Family

The smallest *arachno*-polyborane is $B_2H_7^{-}$[71] (Figure 29) wherein each boron is arbitrarily considered to be associated with two endo-hydrogens and one 5''5''-bridge hydrogen. There are several alkyl derivatives of the isoelectronic and isostructural cation $C_2H_7^+$,[72] as
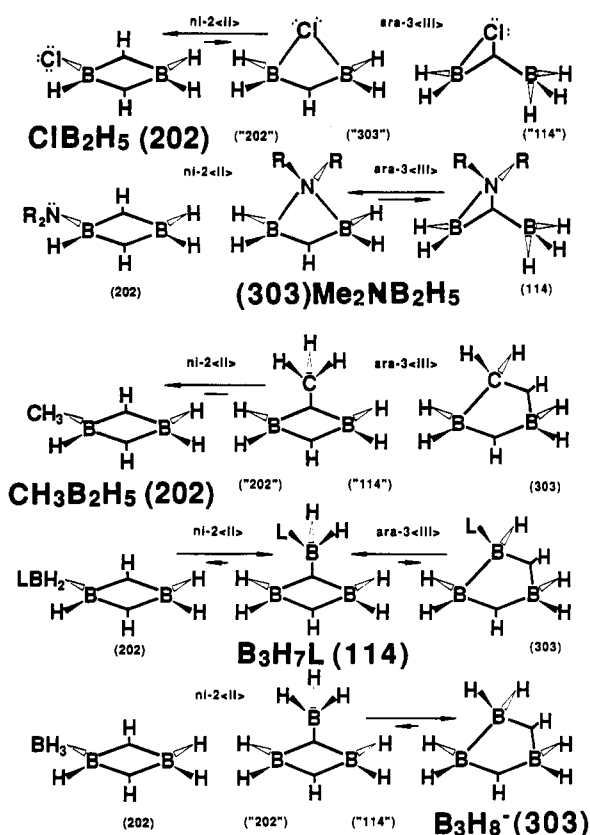
ClB₂H₅ (202)   ("202")   ("303")   ("114")

(303)Me₂NB₂H₅   (202)   (114)

CH₃B₂H₅ (202)   ("202")   ("114")   (303)

B₃H₇L (114)   (202)   (303)

B₃H₈⁻(303)   (202)   ("202")   ("114")

Figure 30. Arachno-2-vertex (Stx = 202) versus arachno-3-vertex (Stx = 303 or 114) structures; 2 B or Not 2 B, that is the question?

Figure 31. Arachno-3-vertex compounds (303 and 114).

2-norbornyl carbocation   B₂H₆ (202)   [B₃H₉] (303)

MeC₂BH₇⁺ (303)   (114)   Hydroboration Rearrangement (303)

well as an alkyl derivative of $B_2H_7^-$ [73] with a bridging methylene group (-RCH-).

Our practice now and in the past, has been to excise any electron-precise alkyl groups (R-), methylene groups (-CR₂-), or methyne groups (-CR<) and to replace them (notionally) with terminal hydrogens in order to focus upon and to categorize only the electron-deficient core-cluster. Thus, the alkyl derivative of arachno-CB₂H₇⁻ (top of Figure 29) may be considered either as an arachno-2-vertex compound (Stx = 104) by excising the methylene moiety or conversely as an arachno-3-vertex compound (Stx = 303). Currently, we list such compounds under both headings, assuming it is better to live with redundancy than to take the chance of missing such compounds in future compilations.

This potential confusion highlights another problem. In Figure 30 are summarized a number of compounds which could have hypothetically assumed either a nido-B₂H₆-related structure (202) or an arachno-[B₃H₉]-related structure (303 or 114).

B. Arachno-3-Vertex Family

At the top of Figure 30, are two rows of optional structures involving groups with lone pairs of electrons available for potential donation, e.g., Cl and NR₂. nido-ClB₂H₅ [74] assumes the nido-diborane structure (Stx = 202) while R₂NB₂H₅ [75] assumes the arachno-triborane structure (Stx = 303) or a structure related to arachno-B₂H₇⁻ (Stx = 104); [73] see Figure 29.

The bottom three rows of Figure 30 compare isoelectronic compounds with no lone pairs of electrons. Only nido-CH₃B₂H₅ [76] assumes what is clearly the diborane-like structure (202).

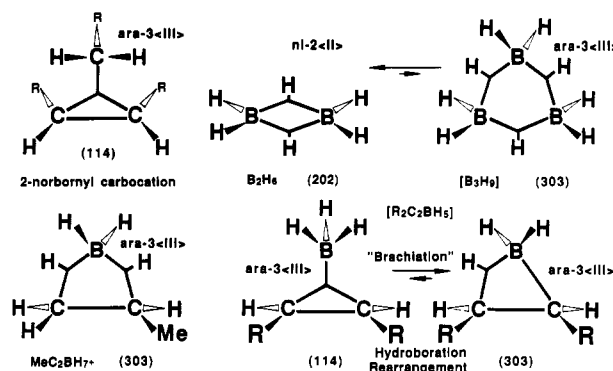The LBH₂ group of B_3H_7L, [77] which is isoelectronic with the H₃C group, favors an alternate bridging configuration (Stx = 114). Another moiety, the H₃B⁻ group in the $B_3H_8^-$, [78] is also, in principle, isoelectronic with the H₃C group; it also "bridges" but favors the Stx = 303 configuration over the 114 structure. This same structural trend is seen upon comparing 2-CH₃B₅H₉ with B₆H₁₀L and B₆H₁₁⁻ (see Figures 16 and 34).

Both R₂NB₂H₅ and B₃H₈⁻ are fluxional under certain conditions and the scrambling of their five and eight hydrogens, respectively, is presumed to go by way of equilibration involving the less-favored alternative 303 and 114 structures.

As many known compounds are related to the arachno-[B₃H₉] family, one wonders why nido-B₂H₆ is stable (Figure 1) rather than the alternative arachno-B₃H₉ (Figure 31) and whether a comparison of their bridge and endo-hydrogen stabilities (Figure 28) could shed any light on the problem.

The Pale Scale (Figure 28) reveals that the limit for neutral nido-B₂H₆ is a restrictive 17 in comparison to a more forgiving value of 23 for neutral arachno-B₃H₉. To be near the pale is undesirable and to go beyond or above the pale invites instability if we subscribe to the speculative, empirically derived hierarchy of architectural features described in Figure 28.

A comparison of the skeletal-hydrogen stabilities, as illustrated in Figure 28 for both nido-B₂H₆ and arachno-B₃H₉, are summarized below:

pale = 17			pale = 23		
nido-B₂H₆ (202)			arachno-B₃H₉ (303)		
two 5'5'₁₁-bridge Hₛ	=	8	three 6'6'₂₂-bridge Hₛ	=	20
	=	8			= 20
two 2-5₁-endo-Hₛ	=	5			= 20
	=	5	three 2-6₂-endo-Hₛ	=	14
					= 14
					14
ave	=	6.5	ave		= 17
spread	=	3 ←	spread		= 6
individual safety margin (ISM)	=	9 ←	ISM		= 3
average safety margin (ASM)	=	10.5 ←	ASM		= 6

The penalties of higher coordination numbers are seemingly apparent. In spite of the more forgiving pale value for neutral arachno-compounds of 23 versus the value for neutral nido-compounds of 17, the skeletal hydrogens in nido-B₂H₆ are at a safer distance from the pale (17 - 8 = 9) while closer to the pale (23 - 20 = 3) in the hypothetical arachno-B₃H₉. Of course this ex-
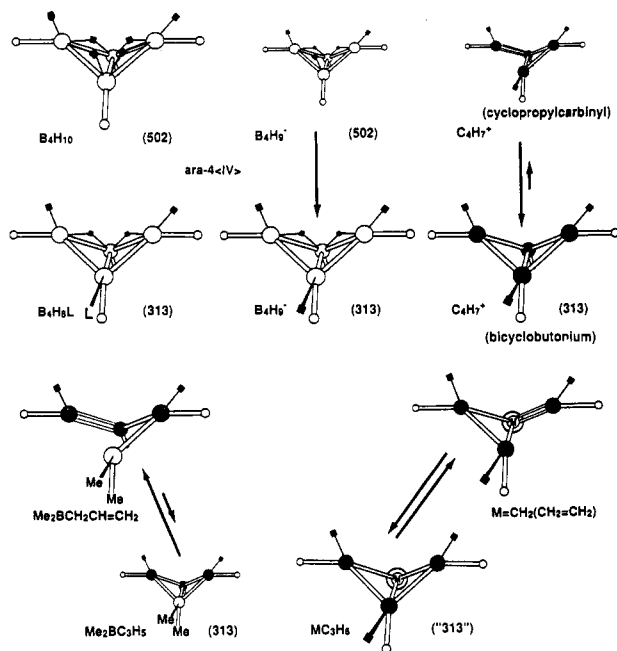
Figure 32. Arachno-4-vertex compounds (502 and 313).

ercise is more a test of the empirical relationships in Figure 28 than a serious attempt to explain why B_2H_6 is more stable than B_3H_9.

In another test case, the long-favored arachno-$B_3H_8^-$ structure[78] (Stx = 303) is estimated to be superior to the alternative structure (Stx = 114) (Figure 30), as would be expected.

<center>pale = 23</center>

arachno-$B_3H_8^-$ (114)		arachno-$B_3H_8^-$ (303)	
two 3-5$_2$-endo-H$_s$	= 22	two 6'5'$_{22}$-bridge H$_s$	= 16
	= 22		= 16
one 5'5'$_{22}$-bridge H	= 12	one 2-6$_2$-endo-H	= 14
two 2-5$_2$-endo-H$_s$	= 8	two 2-5$_2$-endo-H$_s$	= 8
	= 8		= 8
ave	= 14.4 → ave	= 13.6
spread	= 14 → spread	= 8
ISM	= 1 → ISM	= 7
ASM	= 8 → ASM	= 9

The 2-norbornyl carbocation[79] prefers a Stx = 114 configuration rather than the 303 alternative. An alkyl derivative of $C_2BH_8^+$ [80,81] opts for the 303 configuration while the presumed intermediates in hydroboration and the hydroboration (brachiation)[82] rearrangements are presumed to involve both 114 and 303 configurations.

C. Arachno-4-Vertex Family

In Figure 32, the structure of arachno-B_4H_{10} (502)[83] is compared with that of arachno-$B_4H_9^-$ (313).[84] arachno-B_4H_{10} has no reasonable structural alternative to the 502 structure but arachno-$B_4H_9^-$ could conform to either the 502 or the 313 configuration. The Stx = 313 option (observed) is favored on the basis of the larger individual safety margin (17 for 313 versus 14 for 502).

The two CH_2 groups in dimethylallylborane[85a] scramble on an NMR time scale; an intermediate with a 313 configuration is probably involved in this rearrangement. Intermediates in olefin metathesis and in ROMP-polymerization[85b] are also probably isoelectronic with the 313 configuration. The nonclassical $C_4H_7^+$ [86]
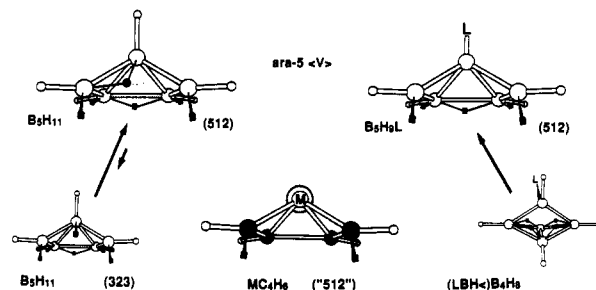

Figure 33. Arachno-5-vertex compounds (512 and 323).

carbocation and isoelectronic $B_4H_8L^{87}$ both have 313 structures.

D. Arachno-5-Vertex Family

The two perennially competitive structures for arachno-B_5H_{11} are displayed, Stx = 512 and 323 (Figure 33). The ^{11}B NMR data was considered for several decades to be compatible only with the 512 configuration;[88] however, the 512 structure was in contradiction to earlier X-ray determinations[89] which favored the 323 configuration. Recent X-ray data[90a] confirm the 512 structure, as does electron diffraction.[90b] Schleyer has confirmed and refined the dimensions of the 512 structure with the ab initio/IGLO/NMR procedure.[91] It is interesting that our Pale Scale assessment (Figure 28) is also ambiguous in the case of B_5H_{11}, but the significantly greater individual safety margin (ISM) of the 512 configuration appears dominant.

<center>pale = 23</center>

arachno-B_5H_{11} (512)		arachno-B_5H_{11} (323)	
one 6'6$_{24}$-bridge H	= 18	one 2-6$_4$-endo-H	= 22
one 6'6$_{23}$-endo-H	= 16	one 66$_{33}$-bridge H	= 12
one 2-6$_2$-endo-H	= 14	two 5'6$_{23}$-bridge H	= 11
one 66$_{33}$-bridge H	= 12		= 11
one 5'6$_{23}$-bridge H	= 11	two 2-5$_2$-endo-H	= 8
one 2-5$_2$ endo-H	= 8		= 8
ave	= 13.2 → ave	= 12
spread	= 10 ← spread	= 14
ISM	= 5 ← ISM	= 1
ASM	= 10 → ASM	= 11

For neutral arachno-compounds the pale value is 23 in Figure 28. The six skeletal hydrogens all have similar values in both the 512 and 323 isomers. The critical difference is the 2-6$_4$-endo-hydrogen (value = 22) in the 323 isomer, which is almost on the pale, if not beyond the pale for neutral arachno-compounds, and thus is indicative of instability.

Kodama has reported the Lewis base adduct arachno-B_5H_9L (L = Me_3P),[92] wherein the LB group (isoelectronic with a CH group) is located at the apex vertex which is nonadjacent to bridge hydrogens (Stx = 512).

The space isomer structure of B_5H_9L (L = 2,6-dimethyllutadene), which may be labeled as a B_4H_{10} derivative (502) with a bridging electron-precise –BHL– group (isoelectronic with –CH_2–), is probably involved in the rearrangement of 1-MeB_5H_8 to 2-MeB_5H_8.[93]

Metallaorganic complexes of butadiene probably have 512-like structures.

E. Arachno-6-Vertex Family

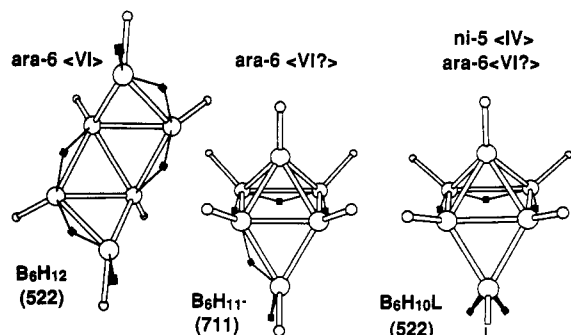Several candidate structures for arachno-B_6H_{12} were projected by Lipscomb;[94] the correct one was later de-

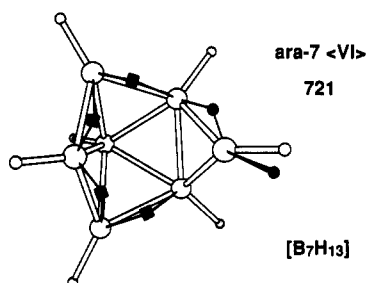**Figure 34.** Arachno-6-vertex compounds (711 and 552).

Figure 35. Arachno-7-vertex compound.

duced from ^{11}B NMR spectra by Gaines and Schaeffer[95] (Figure 34). The structure was reconfirmed by electron defraction by Greenwood et al.[95] and dimensionally refined by Schleyer (ab initio/IGLO).[96] Kodama[97] has prepared the adduct of Me_3P and B_6H_{10} to produce a compound that can be viewed either as arachno-$B_6H_{10}L$ (522) or as nido-(μ-LBH_2)B_5H_8 (610); see parallel situation in Figure 30, i.e., arachno-B_3H_7L (114) or nido-(μ-LBH_2)B_2H_5 ("202").

Shore has prepared $B_6H_{11}^{-}$[98] from $B_5H_8^{-}$[99] and B_2H_6. arachno-$B_6H_{11}^{-}$ has at least two different structures, as reflected in the quite different ^{11}B NMR spectra at different temperatures. We suspect one is the 711-structure proposed by Shore et al.[98] and the other is probably a 522 structure based upon assessment via Figure 28.

F. Arachno-7-Vertex Family

Sneddon has prepared a compound B_7H_{13} that appears to be a fused nido-B_5H_8 (610) moiety bridging or replacing a bridge hydrogen in a nido-B_2H_6 (202).[100] An alternative arachno-721 structure was anticipated[19] (ara-7⟨VI⟩ in Figure 6) and it appears to have the boron arrangement proposed by Shore et al.[5a,10b,10c] for their arachno-$B_7H_{12}^{-}$ and perhaps its $Fe(CO)_4$ adduct. As their proposed structure for arachno-$B_7H_{12}^{-}$ has two endo-hydrogens, Stx would equal 532 rather than 721 (Figure 35).

G. Arachno-8-Vertex Family

Alternative 920, 731, and 542 structures for B_8H_{14}[101] are displayed in Figure 36.

Assessment via Figure 28 suggests that all three, 920, 731 and 542, configurations for arachno-B_8H_{14} are nearly equivalent. We interpret Moody and Schaeffer's ^{11}B NMR evidence as favoring either fluxional pairs of 542 isomers or fluxional sets of 731 and 542 isomers. Sneddon has isolated an arachno-$C_2B_6H_{12}$[102] and as-
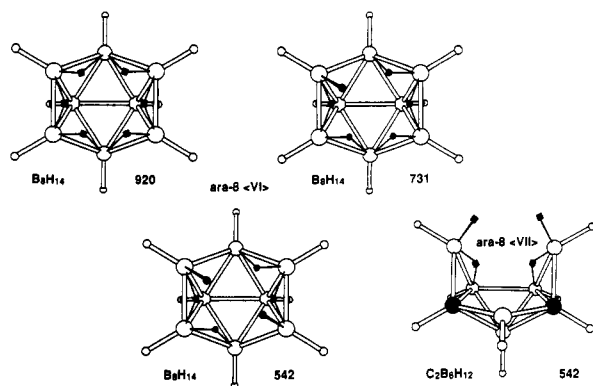
Figure 36. Arachno-8-vertex compounds (920, 731, and 542).
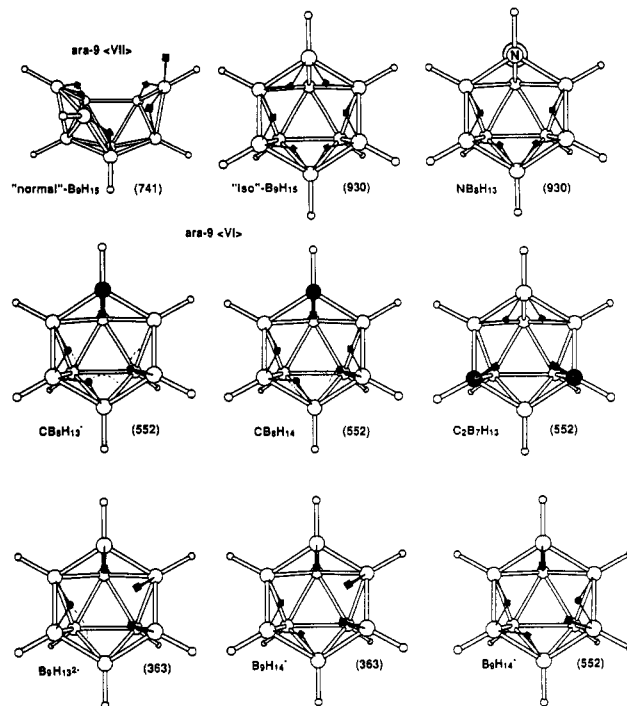
Figure 37. Arachno-9-vertex compounds (930, 741, 552, and 363).

signed to it a 542 structure with a VII-gonal open face. We had expected a 542 structure with a VI-gonal aperture, but Pale Scale assessment via Figure 28 strongly favors Sneddon's proposed structure.

H. Arachno-9-Vertex Family

The arachno-9-vertex compounds are the most prevalent of the arachno-compounds and have the most varied structures (Figure 37). The misnamed (because it was discovered first) normal B_9H_{15} (741)[103] has an ara-9⟨VII⟩ configuration while all other arachno-9-vertex compounds resemble the later discovered i-B_9H_{15}[104] with its ara-9⟨VI⟩ configuration. Four skeletal hydrogen variations are known with zero to three endo-hydrogens, 930, 741, 552, and 363.

Each time an endo-hydrogen (2c2e) is produced, one skeletal BBB 3c2e bond is simultaneously produced. At the same time, one BB (2c2e) and one BHB (3c2e) bond are consumed. In this fashion, the total numbers of 2c2e and 3c2e bonds are conserved.

The S in Stx decreases by 2 while the t and x each gain 1 with each conversion of a bridge hydrogen into an endo-hydrogen. The procedure stops when there are

$$B \overset{H}{\underset{}{\diagdown}} B \qquad \overset{Stx}{\underset{}{930 \rightarrow 741}} \qquad B \qquad \overset{H}{\underset{}{\diagup}} B$$

$$741 \rightarrow 552$$

$$B\underline{\hspace{1cm}}B \qquad 552 \rightarrow 363$$
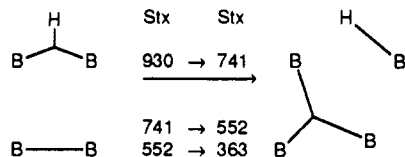
no more pairs of BHB and BB bonds available for conversion into BBB and BH bonds.

Appraisal, via Figure 28, suggests that the six skeletal hydrogens in the aberrant n-B_9H_{15} structure (741)[103] are considerably more stable than in any of the candidate i-B_9H_{15}[104] configurations, and in fact, n-B_9H_{15} is much more stable than i-B_9H_{15}.

Of the four candidate structures (930, 741, 552, or 363) for i-B_9H_{15}, the 930 structure (top–middle in Figure 37) is (a) strongly favored by Pale Scale assessment (an individual safety margin of 5) over the 741 and 552 alternatives (both of which incorporate $76'_{34}$-bridge hydrogens that are beyond the pale for neutral arachno-compounds) and (b) somewhat favored over the best 363 configuration (with an individual safety margin of 3). The ^{11}B NMR data confirm the favored 930 configuration with six bridge hydrogens.

The related $B_9H_{14}^{-}$[105] has the unsymmetrical 363 configuration in the crystal at room temperature but converts to a 552 configuration[106] at -174 °C. Appraisal via Figure 28 marginally favors this 363 configuration on the basis of average safety margin, but other configurations, i.e., 552, 741, and 930, have substantially better individual safety margins of 9 and 11 rather than 7 for the observed 363 structure. Crystal-packing considerations of almost equivalent isomers may select the observed structures and individual safety margins may diminish in importance if all competitive structures are well within the stability limit.

Shore's arachno-$B_9H_{13}^{2-}$[107] in the crystal is a disordered mixture of the 363 structure (shown in Figure 37) and two kinds of 552 structures (not illustrated). The best way to view the randomly cocrystallized isomers is to view the 363 isomer of arachno-$B_9H_{14}^{-}$ (shown) and then to generate the possible isomers of $B_9H_{13}^{2-}$ (363, 552, 552) by the removal of one additional skeletal hydrogen (either bridge or endo) from arachno-$B_9H_{14}^{-}$ on a random basis. The 363 structure of arachno-$B_9H_{13}^{2-}$ in the crystal has an ISM of 13 while the 552 configurations have ISM values of 21; both of the 363 and 552 structures for arachno-$B_9H_{13}^{2-}$ have ISM values so far away from the instability zone that it may not matter. The randomly disordered crystal structure of arachno-$B_9H_{13}^{2-}$ dramatically illustrates the near equivalence of bridge and endo hydrogens and that they define the limits of a continuum with many skeletal hydrogens having properties in between bridge and endo.

The arachno-9-vertex carborane $C_2B_7H_{13}$ has a 552 structure[108] and incorporates two CH_2 groups. The endo-hydrogens are most acidic (labile), as carbon is a three-skeletal-electron donor. When one nitrogen (a four-skeletal-electron donor) replaces the two carbons, e.g., when $C_2B_7H_{13}$ is notionally converted into NB_9-H_{13},[109] an endo-hydrogen might be expected to locate on nitrogen and would, by extension of this trend, be expected to be extremely labile. In fact, the trend goes even further than simple lability of an endo-hydrogen on a hypothetical NH_2 group. The endo-hydrogen
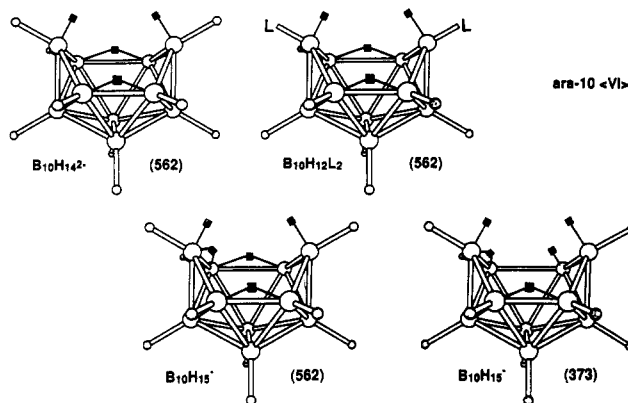

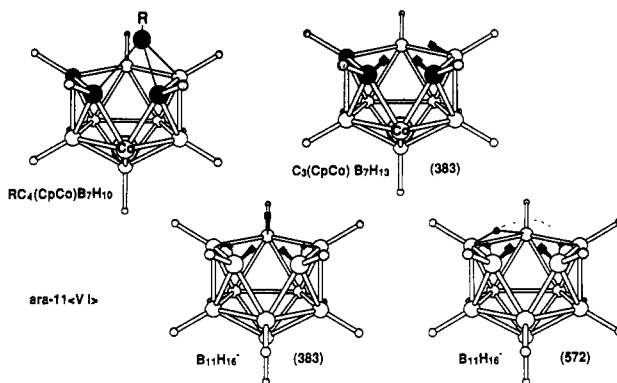**Figure 38.** Arachno-10-vertex compounds.

Figure 39. Arachno-11-vertex compounds (572 vs 383).

(which might have been expected to be located on nitrogen) leaves the nitrogen and relocates on a vacant BB edge position. Thus, a BHB bridge-hydrogen and an NH group are formed rather than an NH_2 group and a vacant BB edge site, e.g., the 930 configuration is produced rather than an NH_2 group and a vacant BB edge site, e.g., the 930 configuration is produced rather than either the 741 or the 552 configurations. See also section I.C. and Figure 2, where a proton may also be thought to leave sulfur (a four-skeletal-electron donor) to become a remote bridge hydrogen.[2,14]

Both arachno-CB_8H_{14} and -$CB_8H_{13}^{-}$ compounds favor fluxional 552 configurations.[109b]

I. Arachno-10-Vertex Family

The known arachno-10-vertex compounds, $B_{10}H_{14}^{2-}$[110] and $B_{10}H_{12}L_2$,[111] have 562 configurations (Figure 38). There is some evidence for the transient existence of an arachno-$B_{10}H_{15}^{-}$ anion. Assessment via Figure 28 predicts that a 373 configuration, with a 2-6_4-endo-hydrogen, would be slightly more stable than a 562 structure which would incorporate a $6'7_{34}$-bridge hydrogen.

J. Arachno-11-Vertex Family

An alkyl and transition element substituted derivative of an arachno-11-vertex compound is known (Figure 39). Following removal of external electron-precise alkyl groups, it should be related to a $C_3(CpCo)B_7H_{13}$ (383) configuration.[112] For comparison, diborane and $B_{10}H_{13}^{-}$ scramble borons in solution in a totally random fashion. An extremely fluxional arachno-$B_{11}H_{16}^{-}$
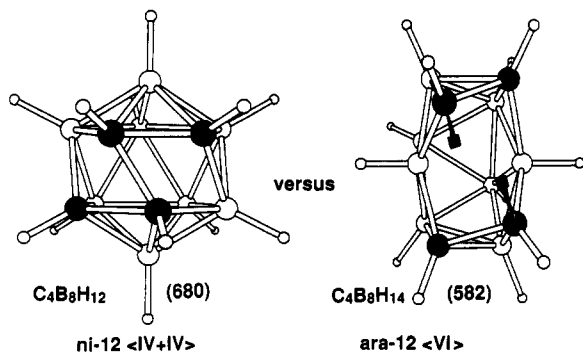
C₄B₈H₁₂ (680)   versus   C₄B₈H₁₄ (582)

ni-12 <IV+IV>   ara-12 <VI>

Figure 40. A candidate arachno-12-vertex configuration (582).

species $(B_{10}H_{13}^- + BH_3)$ is suspecteed to be the active intermediate in ¹⁰B/¹¹B exchange between $B_{10}H_{13}^-$ and B_2H_6.[113] A 383 tautomeric structure for *arachno*-$B_{11}H_{16}^-$ is also favored in this case by Pale Scale assessment. During the preparatioin of this manuscript, Paetzold[113b] revealed an arachno-11-vertex compound containing nitrogen (not shown); it has the projected ara-11⟨VI⟩ configuration.

K. Arachno-12-Vertex Family

We know of only one example of a possible arachno-12-vertex compound (582); it is one isomer of Grimes' *nido*-$R_4C_4B_8H_8$ (680)[64] (Figure 40).

Two trains of thought converge in favor of an ara-12⟨VI⟩ (582) assignment rather than on the nido-12-⟨IV+IV⟩ (680) description for this compound. First, to simplify analysis and bookkeeping, we always followed the practice of notionally removing electron-precise hydrocarbon scaffolding when analyzing the structure of the underlying electron-deficient core-cluster. Thus, we notionally replace endo- or exo-methyl or -ethyl groups with hydrogens prior to cluster analysis. In addition, we also remove -$(CH_2)_n$- groups, e.g., methylene or ethylene groups (where $n = 1$ or 2), and replace them with two endo hydrogens. What about the case where $n = 0$, i.e., where there is an isolated electron-precise 2c2e C–C bond located on the skeletal inner sphere where the skeletal bridge and endo-hydrogens would be expected to reside. We suggest that such a localized electron-precise 2c2e bond should be excised and replaced (Figure 40) by two endo-hydrogens prior to cluster analysis and that Grimes' isomeric form of $R_4C_4B_8H_8$[64] with two neighboring IV-gonal apertures (ni-12⟨IV+IV⟩) might better be viewed as a derivative of *arachno*-$R_4C_4B_8H_8$ with one VI-gonal aperture (ara-12⟨VI⟩).

The second argument is that the same projected arachno-12-vertex configuration for boron, carbon, and hydrogen skeletons is produced from the most spherical closo-14-vertex deltahedron which incorporates two opposed 6 k vertices separated by six pairs of 5 k vertices (Figures 6 and 14). The removal of one of the six pairs of 5 k vertices (between the 6 k vertices) simultaneously reduces both 6 k vertices to 5 k vertices in the resulting arachno-deltahedral fragment (Figure 6). Both approaches converge on the preferred arachno-582 configuration, ara-12⟨VI⟩, displayed in Figures 6 and 40.

Such a reversible nido to arachno interconversion of structures must be very rare, as the atoms would have to be in exactly the right place at the right time and be
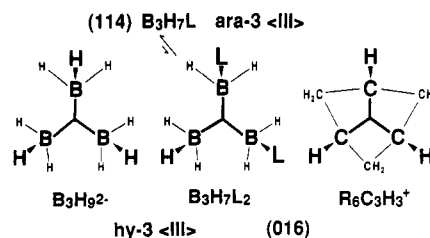
(114) B₃H₇L   ara-3 <III>

B₃H₉²⁻   B₃H₇L₂   R₆C₃H₃⁺
hy-3 <III>   (016)

Figure 41. Hypho-3-vertex compounds (016).
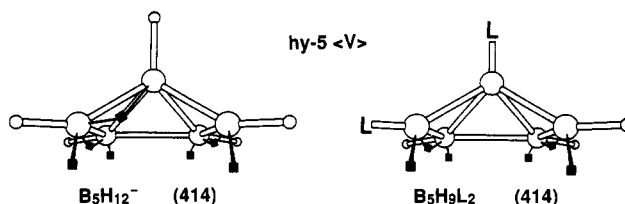
hy-5 <V>

B₅H₁₂⁻ (414)   B₅H₉L₂ (414)

Figure 42. Hypho-5-vertex compounds (414).

sterically constrained so as to be amenable to both structural choices. A second example of a nido to arachno rearrangement has just been reported[113c] (not illustrated).

X. Hypho-Compounds

We are not persuaded that any neutral nonfused *hypho*-polyboranes, B_nH_{n+8}, have ever been isolated, even though B_6H_{14} has been proposed.[114] On the other hand, several hypho-anions and di-Lewis base adducts have been prepared (see below).

A. Hypho-3-Vertex Family

The hypothetical *hypho*-polyborane anion and related *hypho*-carbocation would be $B_3H_9^{2-}$ (016) and $C_3H_9^+$ (016), respectively (Figure 41). Shore may have produced $B_3H_9^{2-}$ as either a stable dianion in solution or as an intermediate.[115] The removal of three -CH_2- groups followed by their replacement with six endo-hydrogens on the trishomocyclopropenium cation[116] would produce *hypho*-$C_3H_9^+$. Paine and Parry have shown that the isoelectronic *hypho*-[$B_3H_7L_2$] must be an intermediate[117] in the boron and hydrogen scrambling in *arachno*-B_3H_7L.

B. Hypho-4-Vertex Family

hypho-$B_4H_8L_2$ (215)[118] might be a hypho-4-vertex compound, but if the pendant BH_2L group is assumed to be electron precise and isoelectronic and isostructural with a CH_3 group, and thus simply replaced with a terminal hydrogen, then it might just as well be considered a derivative of *arachno*-B_3H_7L, i.e., *arachno*-(LBH₂)B_3H_6L (114) (see Figure 32).

C. Hypho-5-Vertex Family

Both *hypho*-$B_5H_9L_2$ (of known X-ray structure[119]) and the isoelectronic[120] *hypho*-$B_5H_{12}^-$ have been reported. The most probable structure of the latter (illustrated in Figure 42) may be extrapolated from the former and its isoelectronic and isostructural resemblance to Hart's carbocation.[121] Schleyer et al.[122] offer ab initio calculations that suggest a configuration similar to the $B_5H_{12}^-$ structure illustrated.
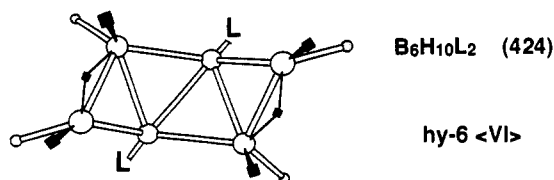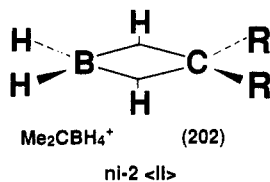
Figure 43. Hypho-6-vertex compounds (424).

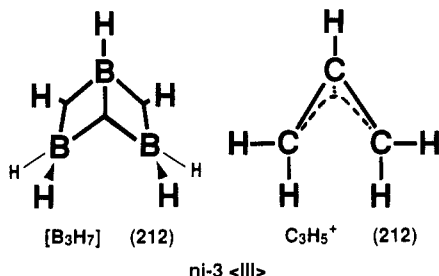**Figure 44.** Nido-2-vertex compounds with endo-hydrogens (202).

Figure 45. Nido-3-vertex compounds with endo-hydrogens (212).

D. Hypho-6-Vertex Family

The di-Lewis base adduct of B_6H_{10}, i.e., $B_6H_{10}L_2$,[123] has been identified and the structure (424) established (Figure 43); hypho-B_6H_{14} has not.

XI. Nido-Compounds (with BH₂ Groups or CH₂ Groups)

Until recently, the presence of BH_2 groups among the larger nido-compounds was not expected. The nido-compounds B_2H_6, $[B_3H_7]$, and $[B_4H_8]$ are simply too small to provide reasonable locations for four skeletal hydrogens without BH_2 groups. The largest, $B_{11}H_{14}^-$ and $B_{11}H_{15}$, nido-compounds accommodate endo-hydrogens (as BH_2 groups) as the lesser of evils when the more offensive alternatives are to incorporate 76-bridge hydrogens in nido-$B_{11}H_{14}^-$ and 77-bridge hydrogens in nido-$B_{11}H_{15}$.

Sneddon has recently isolated one nido-7-vertex compound and one nido-10-vertex compound that also incorporate endo-hydrogens.

A. Nido-2-Vertex Family with Endo-Hydrogens

A carborane cation, $Me_2CBH_4^+$, an analogue of B_2H_6 (202), has been reported based upon ^{11}B NMR data (Figure 44).

B. Nido-3-Vertex Family with Endo-Hydrogens

nido-$[B_3H_7]$ has been postulated as an intermediate (Figure 45) in many reactions and is presumed (by others) to have been produced and to have dimerized into hypho-B_6H_{14}. I suggest nido-B_3H_7 is probably produced as an intermediate and promptly forms the polymer $(B_3H_7)_n$. The best structural choice for monomeric nido-B_3H_7 (ab initio calculations)[29] is compared to the known isoelectronic allyl cation $C_3H_5^+$. They would be isoelectronic but not isostructural.
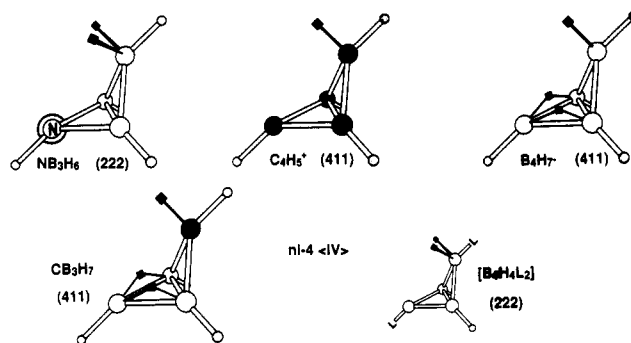

Figure 46. Nido-4-vertex configurations with endo-hydrogens (411 and 222).

C. Nido-4-Vertex Family with Endo-Hydrogens

In 1972, Olah et al. deduced[31] the structure of the first nido-4⟨IV⟩ compound, $C_4H_5^+$ (homocyclopropenium cation), from its ^1H and ^{13}C NMR spectra. Recently (1987), Schindler confirmed[32] Olah's structure via ab initio/IGLO/NMR analysis, which we have further refined (Figure 46).

At that time we did not realize that Olah's $C_4H_5^+$ would be isoelectronic (and probably isostructural) with the reported nido-$B_4H_7^-$ [30] and the reported CB_3H_7[124] although the writer had published extensively[125] (but apparently not exhaustively) on polyborane–nonclassical carbocation isoelectronic and isostructural relationships.

We had used the known structures of several polyboranes and the $^{11}B/^{13}C$ NMR chemical shift relationship[125] to predict and/or confirm a number of nonclassical carbocation structures. We did not think of extrapolating the structures of nido-$B_4H_7^-$ and related compounds from comparisons with Olah's nido-$C_4H_5^+$.[31]

We have compared Olah's cation $C_4H_5^+$ (411) and our ab initio calculated (411) structure for $B_4H_7^-$.[126] The X-ray-determined structure for Paetzold's RNB_3H_5 (222)[127] as well as anticipated structures for Burg's $B_4H_4L_2$[129] and Mattison and Matteschei's CB_3H_7[124] are included.

Most important to the writer is the fact that the electron-deficient ni-4⟨IV⟩ deltahedral fragment structure (either 411 or 222) is derived by the removal of one highest coordinated vertex from the most spherical 5-vertex closo-deltahedron in a direct extension of our original geometrical systematics[2,9] of 1971 (Figure 6) rather than an aberrant tetrahedral fragment configuration favored by others.[130]

D. Nido-7-Vertex and Nido-10-Vertex Families with Endo-Hydrogens

Sneddon's 7-vertex compound nido-$C_2B_5H_8^-$ [27] incorporates an endo-hydrogen (441) rather than a bridge hydrogen (630), for which we have no explanation (Figure 47). Assessment via Figure 28 favors the bridge-hydrogen alternative (630), as it has a safety margin of 14 versus 9 for the 441 tautomer observed. Sneddon's nido-$C_3B_7H_{11}$ (471) derivative[131] incorporates an endo-hydrogen on a CH_2 group, which we believe is the result of the three carbon's positions effectively eliminating any favorable location for a BHB bridge hydrogen.
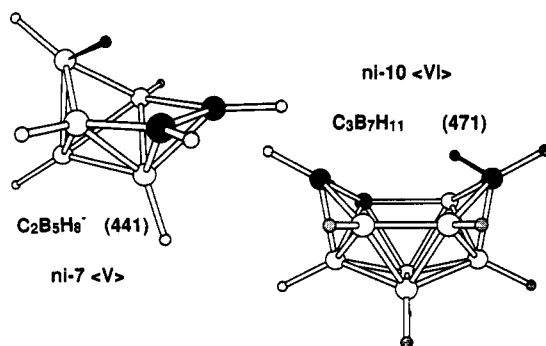
Figure 47. Nido-7- and -10-vertex compounds with endo-hydrogens (441 and 471).
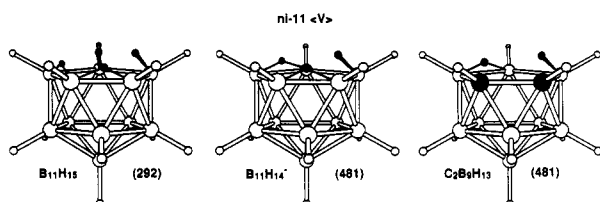

Figure 48. Nido-11-vertex compounds with endo-hydrogens (481 and 292).

E. Nido-11-Vertex Family with Endo-Hydrogens

The V-gonal open face on nido-11-vertex compounds is composed of five borons, each of which is connected to four other borons. $nido$-$B_{11}H_{13}^{2-}$ (670)[60] can accommodate its two skeletal hydrogens with ease as 66_{44}-bridge hydrogens (Figure 22). Figure 28 reveals hierarchy values of 16 for the two bridge hydrogens while the pale is set at 29; thus, there is a very large individual safety margin of 13 for $nido$-$B_{11}H_{13}^{2-}$.

When one more proton is added to $nido$-$B_{11}H_{13}^{2-}$ (670) to form $B_{11}H_{14}^{-}$ (670),[26] with three bridge hydrogens, two destabilizing trends take place in concert: (a) the pale value reduces from 29 to 23, and (b) two 76_{44}-bridge hydrogens are formed with skeletal hierarchy values of 20 (Figure 48). Alternatively, the additional proton could be added as an endo-hydrogen producing the $B_{11}H_{14}^{-}$ tautomer (481), as observed in the crystal.[26] Appraisal via Figure 28 slightly favors the 670 tautomer with an ISM of 3, but the observed crystal structure[26] is the 481 tautomer with an ISM value of 1. As $B_{11}H_{14}^{-}$ is fluxional in solution, probably both 481 and 670 tautomeric structures are involved during rearrangement.

$$B_{11}H_{14}^{-}$$

	670		481
ISM	3	←	1
ASM	3	→	3.5
spread	4	←	6

$nido$-7,8-$C_2B_9H_{13}$[132] probably has a structure emulating $B_{11}H_{14}^{-}$ (481), but if one carbon migrates into a cage site, then the alternative structure (670) in Figure 22 would be observed.

Adding another proton to $nido$-$B_{11}H_{14}^{-}$ to produce $nido$-$B_{11}H_{15}$[27] becomes even more disputatious; the pale for neutral $nido$-polyboranes lowers from 23 to 17, and no matter how the four congested skeletal hydrogens are placed about the open face, all four skeletal hydrogens have hierarchy values well beyond the pale. $nido$-$B_{11}H_{15}$ has been made by Shore at very low temperatures, but it cannot be brought up to a high enough
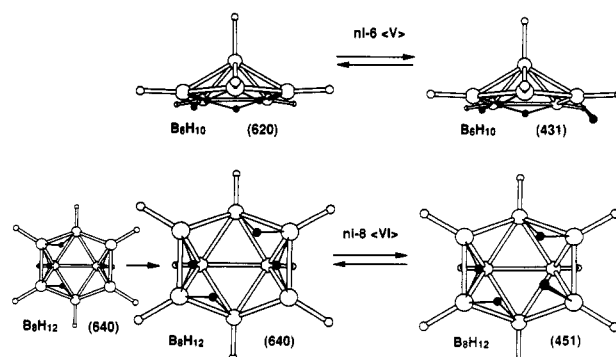

Figure 49. $nido$-B_6H_{10} and $nido$-B_8H_{12} configurations without BH_2 groups are only slightly favored (620 ≥ 431 and 640 ≥ 451).

temperature for either X-ray or ^{11}B NMR analysis without extensive decomposition.

		$B_{11}H_{15}$			
	670		481		292
ISM	$(-7)_2$	→	−7	→	−5
ASM	−5	→	−4.5	→	−4
spread	4	=	4	→	2

On balance, it appears that a 292 configuration should be favored with an ISM of −5 and there is a structural precent for the 292 derivative,[2] e.g., where there are two endo-groups on a nido-11-vertex fragment.

F. Stability of Polyboranes Possibly Linked to the Absence of Endo-Hydrogens (BH₂ Groups)

In general, $nido$-polyboranes (without BH_2 groups) are kinetically more stable than $arachno$-polyboranes (with BH_2 groups). For example, the nonfluxional nido-species B_5H_9 (610) and $B_{10}H_{14}$ (660) are very stable while, in contrast, the fluxional (on an NMR time scale) $nido$-polyboranes B_6H_{10} (620) and B_8H_{12} (640) are as unstable as many $arachno$-polyboranes.

In the past the fluxionality in $nido$-B_6H_{10} and $nido$-B_8H_{12} has been explained (perhaps correctly) as resulting from the availability of neighboring vacant B–B bonds of potentially equivalent coordination numbers if the bridge hydrogens moved from B–B bond to B–B bond. Such situations are not available in $nido$-B_5H_9, as there are no vacancies, nor in $nido$-$B_{10}H_{14}$, as the vacancies that do exist are less favorable.

A second possibility (perhaps complementary) now arises, as none of these four nido-species incorporate BH_2 groups (^{11}B NMR); could there be unobserved structural tautomers of B_6H_{10} (e.g. 431) and B_8H_{12} (e.g. 451) that are almost as stable as the 620 and 640 tautomers and could account for the lack of stability of both B_6H_{10} and B_8H_{12} and their fluxionality?

Assessment via Figure 28 was carried out on both the known 620 and unknown 431 forms of B_6H_{10} and the known 640 and unknown 451 configurations of B_8H_{12} (Figure 49) with the following results:

	B_8H_{12}				B_6H_{10}		
	640	640	451		620		431
	(x-ray)	(NMR)					
ISM	3	= 3	= 3		5	≡	4
ASM	6.8	≅ 6.5	≅ 6.3		6.5	≅	6.3
spread	13	→ 7	= 7		5	≡	6

In both cases, B_6H_{10} and B_8H_{12}, there are almost equivalent isomers with BH_2 groups (431 and 451) and
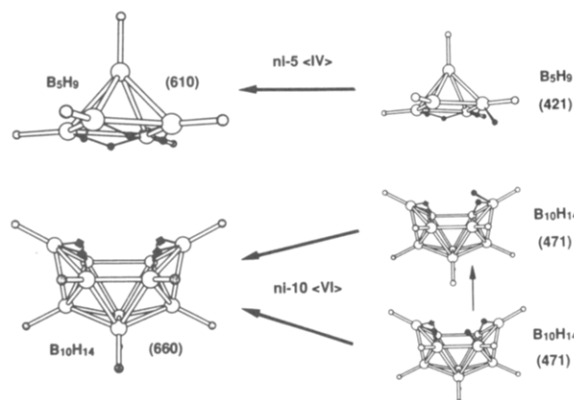
Figure 50. $nido$-B_5H_9 and $nido$-$B_{10}H_{14}$ configurations without BH_2 groups are heavily favored ($610 \gg 421$ and $660 \gg 471$).

without BH_2 groups (620 and 640), and both compounds are highly fluxional, probably using the unobserved 431 and 451 tautomers as intermediates.

For completeness, we carried out similar Pale Scale assessments via Figure 28 on the known 610 and unknown 421 configurations (Figure 50) of the very stable nonfluxional $nido$-B_5H_9 and the known 660 and two variations of unknown 471 configurations of the very stable nonfluxional $nido$-$B_{10}H_{14}$. The results were dramatically different:

	B_5H_9		$B_{10}H_{14}$		
	__610__	421	__660__	471	471
				(6-endo)	(5-endo)
ISM	+5	← −1	+3	← −3	← −5
ASM	+5	→ 5.2	+3	← +0.5	→ +2.3
spread	0	← 11	0	← 6	← 13

In both cases, $nido$-B_5H_9 and $nido$-$B_{10}H_{14}$, the unobserved potential 421 and 471 tautomers, would incorporate skeletal hydrogens that are beyond the pale for neutral nido-compounds while the known 610 and 660 tautomers have substantial individual safety margins. Perhaps it is understandable that the 421 and 471 tautomers are not observed and that both B_5H_9 and $B_{10}H_{14}$ are stable and not fluxional on an NMR time scale at ambient conditions.

In contrast, the 610 and 421 tautomers of $nido$-$B_5H_8^-$ are almost equivalent by Pale Scale analysis and $B_5H_8^-$ is much less stable than B_5H_9 and fluxionality is known to be prevalent (^{11}B NMR). Fluxionality thus seems to be coupled to less thermal stability, but whether it is preevented by unacceptable BH_2-containing tautomers or promoted by equivalent neighboring vacancies remains unanswered.

All four neutral nido-compounds, B_5H_9, B_6H_{10}, B_8H_{12}, and $B_{10}H_{14}$, exhibit the same ^{11}B NMR spectra at ambient conditions whether they are neat or in a wide variety of solvents. While B_5H_9 and $B_{10}H_{14}$ are stable indefinitely, both B_6H_{10} and B_8H_{12} decompose in minutes to hours if stored neat but store indefinitely if kept in diethyl ether. We suggest that both $nido$-B_6H_{10} and $nido$-B_8H_{12} probably decompose via their transient 431 and 451 tautomers, which are rapidly (and reversibly) sequestered as the more stable $arachno$-$B_6H_{10}OEt_2$ and $arachno$-$B_8H_{12}OEt_2$ species when either is the diluent. It would be revealing if $nido$-$B_5H_8^-$ were stabilized by ethers.

When a stronger Lewis base such as Me_3P is present, B_6H_{10} forms $arachno$-$B_6H_{10}PMe_3$ (Figure 37).

XII. Summary and Future Implications

A. Electron-deficient compounds assume structures based on deltahedra and deltahedral fragments.

B. Greater electron deficiency leads to more connections between skeletal vertices.

C. Various groups contribute skeletal electrons to electron-deficient deltahedra or deltahedral fragment clusters. Groups have been identified that donate from −2 to +4 skeletal electrons (−2 skeletal-electron donors are identified as −2 EDs while +4-skeletal-electron donors are labeled 4 EDs).

D. Those deltahedra and deltahedral fragment structures characteristic of the polyboranes, carboranes, and carbocations are based upon the most spherical deltahedra (Figure 6) because such skeletons are composed of vertices which differ least in their connectivities. Such vertices are optimal for atoms or groups that differ least in their capacities as electron donors. In contrast to all alternative deltahedra, the most spherical deltahedra incorporate vertices with the narrowest possible ranges of connectivities, generally 4 k and 5 k vertices (rarely, 3 k and 6 k vertices), which matches the narrow range of electron donor capacities, e.g. 2 ED and 3 ED, for the BR and CR groups occupying those vertices.

E. Those groups donating the most electrons in the carboranes are the CH or CR groups (3 EDs), which, in response to charge-smoothing driving forces, preempt the most electron-rich environments, in the order 3 k > 4 k > 5 k. The result is that the carbons are found in the lowest coordinated sites available, about the various deltahedra or deltahedra fragments, surrounded by lesser electron donors, i.e., the BR groups (2 EDs). This latter feature also accounts for the carbons being separated in the thermodynamically most stable isomers if other geometrical considerations are equivalent.

F. When the electron-donating groups vary in their electron-donating capacities by two electrons, in susceptible nido-deltahedral fragments, e.g., RN (4 ED) versus RB (2-ED), the RN groups, which may be considered to have been forced to donate the larger number of electrons to the total number of skeletal electrons (greater donors), tend to induce the global electron density back toward the greater donating groups, causing the skeletal-electron distribution to become more concentrated about the RN groups and incrementally diminished around the RB groups. As a result, the immediate environment around the one or two greater donors (4 ED, RN groups) may be considered to be less electron deficient or incrementally more electron precise while the surroundings of the greater number of lesser donors (e.g., the RB groups) tend to become incrementally more electron deficient.

As greater electron deficiency spawns more connections (Figure 1), an additional connection is added when geometrically practicable and the open faces of such nido-compounds may become smaller. A quite different deltahedral fragment of the most spherical parent deltahedron is frequently or usually observed ($N_2B_4H_6$ vs $2,4$-$C_2B_4H_6^{2-}$ in Figure 17).

G. When the electron-donating capacity of the various groups within a given cluster differs by three or more electrons, an entirely different deltahedron with much less homogeneously connected vertices may be chosen rather than the most spherical deltahedra, which

tend to incorporate the most homogeneously connected vertices. As only one example, Cotton's closo-$(L_2:Hfl_2)_2C_6H_6$ compound (L = PR_3) adopts[128] an alternative closo-8-vertex dodecahedral structure. The hexagonal bipyramid configuration with two 6 k vertices and six 4 k vertices is adopted by closo-$(L_2:Hfl_2)_2C_6H_6$ rather than the most spherical bisdisphenoid (characteristic of closo-$C_2B_6H_8$; Figure 11), which contains equal numbers of 4 k and 5 k vertices. The $L_2:Hfl_2$ groups (0 EDs) occupy the two opposed 6 k vertices while the six carbons (3 EDs) occupy the six 4 k vertices in the hexagonal bipyramid). In this case, the much less uniform vertices (6 k versus 4 k) efficiently match and accommodate the much less uniform ED values (0 ED versus 3 ED).

An even more extreme example is found in nido-$(C_8H_8)_2U$,[133] which assumes a nido-9-vertex octagonal pyramidal structure which incorporates one 8 k vertex and eight 3 k vertices. It is derived from the closo-10-vertex octagonal bipyramid, by the removal of one 8 k vertex, rather than by the removal of a 5 k vertex from the most spherical closo-10-vertex bicapped Archimedean antiprism characteristic of the carboranes. The eight carbons in the C_8H_8 ring (3 EDs) donate three electrons apiece and occupy the matching eight 4 k sites while the "other" C_8H_8U group "donates" minus two electrons (–2 ED) and occupies the lone remaining 8 k site! The CH and C_8H_8U groups differ greatly in their electron-donating capacities (–2 ED versus 3 ED) and thus ideally occupy sites which differ widely in their connectivity (4 k versus 8 k). For bookkeeping purposes, two 4c2e bonds may be considered to be involved in nido-$(C_8H_8)_2U$.

H. To date, all arachno and hypho-compounds seem to adopt most spherical deltahedral fragment structures when 2 ED, 3 ED, and 4 ED skeletal groups are involved. The differences in donating capacities are seemingly accommodated by having different numbers of bridge and endo-hydrogens in the vicinity of the various groups as a function of their electron-donating capacities. For example, boron groups (2 EDs) neighbor both endo- and bridge hydrogens (≤7 coordinate) while carbon groups (3 EDs) reduce their connectivity (≤6 coordinate) by neighboring only endo-hydrogens (almost never bridge hydrogens), and nitrogen groups (4 ED) tolerate neither endo nor bridge hydrogens in arachno- and hypho-environments and thus lower their connectivity even further (≤5 coordinate).

It is anticipated that when arachno- and hypho-compounds incorporating groups with even greater divergences in their capacities to donate electrons to their global skeletal electron pools are identified or discovered, we will find that nature adopts other strategies and/or other deltahedral fragments to accommodate these differences. Compounds illustrating these points have probably already been reported and have simply not been recognized.

XIII. Acknowledgment

XIV. References

(1) *Electron Deficient Boron and Carbon Clusters*; Olah, G. A., Wade, K., Williams, R. E., Eds.; John Wiley and Sons: New York, 1991.
(2) Williams, R. E., see Chapter 2 of ref 1.
(3) (a) Espoused at a lecture at Cal Tech in the early 1950s by either the speaker or a member of the audience (both forgotten). (b) Brought to the attention of the author by referee #1: there could be a third tautomer associating the RS group to the two borons by a 3c2e bond (isostructural with diborane) which would further increase charge smoothing. Apparently access to the minimum number of 3c2e bonds is more important to the electronegative sulfur than the increased charge smoothing. The coexistence of lone pairs (1c2e) and 3c2e bonds on the same atom is known but not when easy alternatives are possible.
(4) Tippe, A.; Hamilton, W. C. *Inorg. Chem.* **1969**, *8*, 464.
(5) (a) Remmel, R. J.; Johnson, H. D.; Jaworiwsky, I. S.; Shore, S. G. *J. Am. Chem. Soc.* **1975**, *97*, 5395. (b) Olah, G. A.; Prakash, G. K. S.; Williams, R. E.; Field, L. D.; Wade, K. *Hypercarbon Chemistry*; Wiley-Interscience: New York, 1987.
(6) (a) Lipscomb, W. N. *Boron Hydrides*; Benjamin: New York, 1963; p 43. (b) styx for nido-B_5H_9 = 4120: 4 = BHB bonds, 1 = BBB bonds, 2 = BB bonds, and 0 = BH_2 groups (see Figure 4).
(7) (a) Wade, K. *Adv. Inorg. Chem. Radiochem.* **1976**, *18*, 1. (b) Wade, K. *J. Chem. Soc. Chem. Commun.* **1971**, 792.
(8) Williams, R. E. *Adv. Inorg. Chem. Radiochem.* **1976**, *18*, 67.
(9) Williams, R. E. *Inorg. Chem.* **1971**, *10*, 210.
(10) (a) Deltahedra are polyhedra composed exclusively of triangular (Δ) facets. (b) Johnson, H. D.; Shore, S. G. *J. Am. Chem. Soc.* **1971**, *93*, 3798. (c) Mangion, M.; Claton, W. R.; Hollander, O.; Shore, S. G. *Inorg. Chem.* **1977**, *16*, 2110.
(11) Figure 61 of ref 2.
(12) Venable, T. L.; Maynard, R. B.; Grimes, R. N. *J. Am. Chem. Soc.* **1989**, *106*, 6187.
(13) Paetzold, P.; Muller, A. H. E.; Runsink, J. *Angew. Chem.* **1991**, *103*, 201.
(14) (a) Mielcarek, J. J.; Keller, P. C. *J. Chem. Soc., Chem. Commun.* **1972**, 1090. (b) Mielcarek, J. J.; Keller, P. C. *J. Am. Chem. Soc.* **1974**, *96*, 7143.
(15) (a) Onak, T. P.; Drake, R.; Dunks, G. *J. Am. Chem. Soc.* **1965**, *87*, 2505. (b) Prince, S. R.; Schaeffer, R. O. *J. Chem. Soc., Chem. Commun.* **1968**, 451. (c) McKown, G. L.; Don, B. P.; Beaudet, R. A.; Vergamini, P. J.; Jones, L. H. *J. Am. Chem. Soc.* **1976**, *98*, 6909.
(16) (a) Kuznetsov, N. T.; Solntsev, K. A.; Poster #11 at IMEBORON-VII, Torun, Poland, July 30 to Aug 3, 1990. (b) Mennekes, T.; Paetzold, P., personal communication from P. Paetzold to R. E. Williams on October 1, 1991.
(17) (a) Williams, R. E.; Good, C. D.; Shapiro, I. Abstracts of the 140th Meeting of the American Chemical Society, Chicago, IL, 1961; 14 N, p 36. (b) Good, C. D.; Williams, R. E. U.S. Patent No. 3030289 (1959); *Chem. Abstr.* **1962**, *57*, 12534b. (c) Hosmane, N. S.; Barreto, R. D.; Tolle, M. A.; Alexander, J. J.; Quintana, W.; Seriwardand, U.; Shore, S. G.; Williams, R. E. *Inorg. Chem.* **1990**, *29*, 2698.
(18) Williams, R. E.; Gerhart, F. J. *J. Am. Chem. Soc.* **1965**, *87*, 3513.
(19) (a) Berry, T. E.; Tebbe, F. N.; Hawthorne, M. F. *Tetrahedron Lett.* **1965**, *12*, 715. (b) Tebbe, F. N.; Garrett, P. M.; Hawthorne, M. F. *J. Am. Chem. Soc.* **1964**, *86*, 4222. (c) Tsai, C.; Strieb, W. E. *J. Am. Chem. Soc.* **1966**, *88*, 4513.
(20) Lonquet-Higgins, H. C.; Roberts, M. De V. *Proc. R. Soc.* **1955**, *A230*, 110.
(21) Eberhardt, W. H.; Crawford, B. L.; Lipscomb, W. N. *J. Chem. Phys.* **1954**, *22*, 989.
(22) Klanberg, F.; Muetterties, E. L. *Inorg. Chem.* **1966**, *5*, 1955.
(23) Tebbe, F. N.; Garrett, P. M.; Young, D. C.; Hawthorne, M. F. *J. Am. Chem. Soc.* **1966**, *88*, 609.
(24) (a) Bobinsky, J. J. *J. Chem. Ed.* **1964**, *41*, 500. (b) Heying, T. L.; Ager, J. W.; Clark, S. L.; Mangold, D. J.; Goldstein, H. L.; Hillman, M.; Polak, R. J.; Szymanski, J. W. *Inorg. Chem.* **1963**, *2*, 1089. (c) Potenza, J. A.; Lipscomb, W. N. *J. Am. Chem. Soc.* **1964**, *86*, 1874. (d) Potenza, J. A.; Lipscomb, W. N. *Inorg. Chem.* **1964**, *3*, 1673. (e) Schroeder, H.; Vickers, G. D. *Inorg. Chem.* **1963**, *2*, 1317. (f) Grafstein, D.; Dvorak, J. *Inorg. Chem.* **1963**, *2*, 1128. (g) Pepetti, S.; Heying, J. L. *J. Am. Chem. Soc.* **1964**, *86*, 2295. (h) Fein, M. M.; Bobinsky,

J.; Mays, N.; Schwartz, N. N.; Cohen, M. S. *Inorg. Chem.* **1963**, *2*, 1111.

(25) (a) Williams, R. E.; Gerhart, F. J. *J. Am. Chem. Soc.* **1965**, *87*, 3514. (b) Tebbe, F. N.; Garrett, P. M.; Hawthorne, M. F. *J. Am. Chem. Soc.* **1968**, *90*, 869. (c) Parry, R. W.; Edwards, J. L. *J. Am. Chem. Soc.* **1959**, *81*, 3554.

(26) Getman, T. D.; Krause, J. A.; Shore, S. G. *Inorg. Chem.* **1988**, *27*, 2398.

(27) Beck, J. S.; Quintana, W.; Sneddon, L. G. *Organometallics* **1988**, *7*, 1015.

(28) Sang, O. K.; Furst, G. T.; Sneddon, L. G. *Inorg. Chem.* **1989**, *28*, 2339.

(29) McKee, M. L.; Lipscomb, W. N. *Inorg. Chem.* **1982**, *21*, 2846.

(30) Kodama, G.; Parry, R. W. *J. Am. Chem. Soc.* **1972**, *94*, 407.

(31) Olah, G. A.; Staral, J. S.; Spear, R. J.; Liang, G. *J. Am. Chem. Soc.* **1975**, *97*, 5489.

(32) Schindler, M. *J. Am. Chem. Soc.* **1987**, *109*, 1024.

(33) Tucker, P. M.; Onak, T. P.; Leach, J. B. *Inorg. Chem.* **1970**, *9*, 1430.

(34) Franz, D. A.; Grimes, R. N. *J. Am. Chem. Soc.* **1970**, *92*, 1438; **1972**, *94*, 412.

(35) (a) Williams, R. E. *Inorg. Chem.* **1971**, *10*, 210, footnote 7. (b) Stohrer, W. D.; Hoffman, R. *J. Am. Chem. Soc.* **1972**, *94*, 1661. (c) Masamune, S.; Sakai, M.; Ona, H.; Jones, A. J. *J. Am. Chem. Soc.* **1972**, *94*, 8956.

(36) Paetzold, P. In *Boron Chemistry*; Hermanek, S., Ed.; World Sci. Publ. Co. Inc.: Singapore, 1987. Personal communication to R. E. Williams, IMEBORON-VI, Bechyne, Czechoslovakia, June 1987.

(37) Kang, S. O.; Sneddon, L. G. *Inorg. Chem.* **1988**, *27*, 3769.

(38) (a) Williams, R. E.; Bausch, J. W.; Prakash, G. K. S.; Onak, T. P. BUSA-II Metting, Research Triangle Park, NC, June 9, 1990. (b) Hosmane, N. S.; Jia, L.; Zhang, H.; Bausch, J. W.; Prakash, G. K. S.; Williams, R. E.; Onak, T. P. *Inorg. Chem.* **1991**, *30*, 3793.

(39) Hosmane, N. S.; Lu, K.-J.; Cowley, A. H.; Mardones, M. A. *Inorg. Chem.* **1991**, *30*, 1325.

(40) Enrione, R. E.; Boer, P. F.; Lipscomb, W. N. *J. Am. Chem. Soc.* **1964**, *86*, 1451; *Inorg. Chem.* **1964**, *3*, 1659.

(41) (a) Fehlner, T. P. *J. Am. Chem. Soc.* **1977**, *99*, 8355. (b) Fehlner, T. P. *J. Am. Chem. Soc.* **1980**, *102*, 3424. (c) Siebert, W.; El-Essawi, M. E. M. *Chem. Ber.* **1979**, *112*, 1480.

(42) Zimmerman, G. J.; Sneddon, L. G. *Inorg. Chem.* **1980**, *19*, 3650.

(43) (a) Bausch, J. W.; Prakash, G. K. S.; Williams, R. E. Submitted. (b) BUSA-II Meeting, Research Triangle Park, NC, June 9, 1990.

(44) (a) Gotcher, A. J.; Ditter, J. F.; Williams, R. E. *J. Am. Chem. Soc.* **1973**, *95*, 7514. (b) Reilly, T.; Burg, A. B. *Inorg. Chem.* **1974**, *13*, 1250. (c) Figure 2.36 in ref 2.

(45) (a) Briguglio, J. J.; Carroll, P. J.; Corcoran, E. W.; Sneddon, L. G. *Inorg. Chem.* **1986**, *25*, 4621. (b) Figure 2.37 in ref 2.

(46) Zimmerman, G. J.; Sneddon, L. G. *J. Am. Chem. Soc.* **1981**, *103*, 1102.

(47) Kutzelnigg, W. *Isr. J. Chem.* **1980**, *19*, 193.

(48) Schindler, M. *J. Am. Chem. Soc.* **1987**, *109*, 1020.

(49) Schleyer, P. v. R.; Laidig, K. E.; Wiberg, K. B.; Saunders, M.; Schindler, M. *J. Am. Chem. Soc.* **1988**, *110*, 300.

(50) Buehl, M.; Schleyer, P. v. R., Chapter 4, ref 1.

(51) (a) Siedle, A. R. Ph.D. Thesis, Indiana University, Bloomington, IN, 1973; p 61.

(52) Zimmerman, G. J.; Sneddon, L. G. *J. Am. Chem. Soc.* **1981**, *103*, 1103.

(53) (a) Siedle, A. R.; Bodnee, G. M.; Todd, L. J. *J. Inorg. Nucl. Chem.* **1971**, *33*, 3671. (b) Sneddon, L. G.; Huffman, J. C.; Schaeffer, R. O.; Streib, W. E. *Chem. Commun.* **1972**, 474.

(54) Shore, S. G. et al. Submitted.

(55) Stibr, B.; Janousek, Z.; Base, K.; Hermanek, S.; Plesek, J.; Zakharova, I. A. *Collect. Czech. Chem. Commun.* **1984**, *49*, 1891.

(56) (a) Stibr, B.; Hermanek, S.; Janousek, Z.; Plzak, Z.; Dolansky, J.; Plesek, J. *Polyhedron* **1982**, *1*, 822. (b) Stibr, B.; Plesek, J.; Zobakova, A. *Polyhedron* **1982**, *1*, 826.

(57) Stibr, B.; Jelinek, T.; Plesek, J.; Drdakova, E.; Plzak, Z.; Hermanek, S. *J. Chem. Soc., Chem. Commun.* In press.

(58) (a) Koster, R.; Seidel, G.; Wrackmeyer, B.; Blasef, D.; Boese, R. *Chem. Ber.* **1992**, *125*. (b) Koster, R.; Seidel, G.; Wrackmeyer, B. *Angew. Chem.* **1985**, *97*, 317; *Angew. Chem., Int. Ed. Engl.* **1985**, *24*, 326. (c) Koster, R.; Seidel, G.; Horstschaefer, W.; Siebert, W.; Gangmus, B. *Inorg. Synth.* **1991**, *29*.

(59) Greenwood, N. N., Chapter 6, ref 1, 172.

(60) (a) Aftandilian, V. D.; Miller, H. C.; Parshall, G. W.; Muetterties, E. L. *Inorg. Chem.* **1962**, *1*, 734. (b) Fritchie, C. J. *Inorg. Chem.* **1967**, *6*, 1199.

(61) Stibr, B.; Plesek, J.; Jelinek, T.; Base, K.; Janousek, Z.; Hermanek, S. In *Boron Chemistry*; Hermanek, S., Ed.; World Sci. Publ. Co. Inc.: Singapore, 1987.

(62) Astheimer, R. J.; Sneddon, L. G. *Inorg. Chem.* **1983**, *22*, 1928.

(63) Greenwood, N. N., Chapter 6, ref 1, p 175.

(64) Venable, T. L.; Maynard, R. B.; Grimes, R. N. *J. Am. Chem. Soc.* **1984**, *106*, 6187.

(65) Getman, T. D.; Knobler, C. B.; Hawthorne, M. F. *Inorg. Chem.* **1990**, *29*, 158.

(66) Jutzi, P. *J. Organomet. Chem.* **1990**, *400*, 12.

(67) Fricsen, G. D.; Barriola, A.; Daluga, P.; Ragatz, P.; Huffman, J. C.; Todd, L. J. *Inorg. Chem.* **1980**, *19*, 458.

(68) Getman, T. D.; Krause, J. A.; Niedenzu, P. M.; Shore, S. G. *Inorg. Chem.* **1989**, *28*, 1507.

(69) Moody, D. C.; Schaeffer, R. *Inorg. Chem.* **1976**, *15*, 235.

(70) Luo, Y.-R.; Benson, S. W. *J. Phys. Chem.* **1990**, *94*, 914; **1989**, *93*, 7333; **1988**, *92*, 5255.

(71) (a) Gaines, D. F. *Inorg. Chem.* **1963**, *2*, 523. (b) Hertz, R. K.; Johnson, H. D.; Shore, S. G. *Inorg. Chem.* **1973**, *12*, 1875. (c) Shore, S. G.; Lawrence, S. H.; Watkins, M. I.; Bau, R. *J. Am. Chem. Soc.* **1982**, *104*, 7669.

(72) (a) Kirchen, R. P.; Sorensen, T. S. *Chem. Commun.* **1978**, 769. (b) McMurry, J. E.; Hodge, C. N. *J. Am. Chem. Soc.* **1984**, *106*, 6450.

(73) Brown, H. C. *Hydroboration*; W. A. Benjamin Publ.: New York, 1962.

(74) Iijima, T.; Hedberg, L.; Hedberg, K. *Inorg. Chem.* **1977**, *16*, 3230.

(75) Cohen, E. A.; Beaudet, R. A. *Inorg. Chem.* **1973**, *12*, 1570.

(76) (a) Penn, R. E.; Buxton, L. W. *J. Chem. Phys.* **1977**, *67*, 831. (b) Chiu, C.; Burg, A. B.; Beaudet, R. A. *Inorg. Chem.* **1982**, *21*, 1204.

(77) (a) Glore, J. D.; Rathke, J. W.; Schaeffer, R. O. *Inorg. Chem.* **1973**, *12*, 2175. (b) Paine, R. T.; Parry, R. W. *Inorg. Chem.* **1972**, *11*, 268.

(78) (a) Peters, C. R.; Nordman, C. E. *J. Am. Chem. Soc.* **1960**, *82*, 5758. (b) Brellochs, B.; Binder, H. *Naturforsch.* **1988**, *43*, 648.

(79) Olah, G. A.; Prakash, G. K. S.; Williams, R. E.; Field, L. D.; Wade, K. *Hypercarbon Chemistry*; John Wiley and Sons: New York, 1987; pp 160–162.

(80) Williams, R. E.; Prakash, G. K. S.; Field, L. D.; Olah, G. A. *Advances in Boron and the Boranes*; Liebman, J. F., Greenberg, A., Williams, R. E., Eds.; VCH Publishers, Inc.: New York, 1988; Chapter 9, p 222.

(81) (a) Williams, R. E. IMEBORON-III; Munchen-Ettal, 1976. (b) Williams, R. E.; Field, L. D. IMEBORON-IV; Snowbird, UT, 1979, In *Boron Chemistry*; Parry, R. W., Kodama, G., Eds.; Pergammon Press: Oxford, 1980.

(82) (a) Williams, R. E. *Inorg. Chem.* **1962**, *1*, 971. (b) Brown, H. C. *Hydroboration*; W. A. Benjamin: New York, 1962. (c) Rickborn, B.; Wood, S. E. *J. Am. Chem. Soc.* **1971**, *93*, 3940.

(83) (a) Nordman, C. E.; Lipscomb, W. N. *J. Chem. Phys.* **1953**, *21*, 1856. (b) Jones, M. E.; Hedberg, K.; Shomaker, V. *J. Am. Chem. Soc.* **1953**, *75*, 7116. (c) Simmons, N. P. C.; Burg, A. B.; Beaudet, R. A. *Inorg. Chem.* **1981**, *20*, 533.

(84) Johnson, H. D.; Geanangel, R. A.; Shore, S. G. *Inorg. Chem.* **1970**, *9*, 908.

(85) (a) Mikhailov, B. M.; Bubnov, Yu. N. *Organoboron Compounds*; Harwood Academic: New York, 1984. (b) Grubbs, R. H.; Tumas, W. *Science* **1990**, *243*, 907. (c) Piers, W. E.; Bercaw, J. E. *J. Am. Chem. Soc.* **1990**, *112*, 9406. (d) Clawson, L.; Soto, J.; Buchwald, S. L.; Stigerwald, M. L.; Grubbs, R. H. *J. Am. Chem. Soc.* **1985**, *107*, 3377.

(86) Pages 202–204 in ref 80.

(87) Jock, C. P.; Kodama, G. *Inorg. Chem.* **1988**, *27*, 3431.

(88) (a) Williams, R. E.; Gibbins, S. G.; Shapiro, I. *J. Chem. Phys.* **1959**, *30*, 320. (b) Williams, R. E.; Gerhart, F. J.; Pier, E. *Inorg. Chem.* **1965**, *4*, 1239.

(89) Moore, E. B.; Dickerson, R. E.; Lipscomb, W. N. *J. Chem. Phys.* **1957**, *27*, 209.

(90) (a) Huffman, J. C. Ph.D. Thesis, Indiana University, 1974. (b) Greenwood, N. N., Chapter 6, p 167 of ref 1.

(91) Buehl, M.; Schleyer, P. v. R. Chapter 4, p 127 of ref 1.

(92) Mitsuaki, K.; Kodama, G. *Inorg. Chem.* **1982**, *21*, 1267.

(93) (a) Onak, T. P.; Gerhart, F. J.; Williams, R. E. *J. Am. Chem. Soc.* **1963**, *85*, 1754. (b) Kodama, G. *J. Am. Chem. Soc.* **1972**, *94*, 5907.

(94) Lipscomb, W. N., p 57 of ref 6.

(95) (a) Gaines, D. F.; Schaeffer, R. O. *Inorg. Chem.* **1964**, *3*, 438. (b) Greenwood, N. N., Chapter 6, p 166 of ref 1.

(96) Buehl, M.; Schleyer, P. v. R., Chapter 4, pp 117, 128 of ref 1, 1991.

(97) Mitsuaki, K.; Kodama, G. *Inorg. Chem.* **1981**, *20*, 1072.

(98) Remmel, R. J.; Johnson, H. D.; Joworiwsky, I. S.; Shore, S. G. *J. Am. Chem. Soc.* **1975**, *97*, 5395.

(99) (a) Onak, T. P.; Dunks, G. B.; Searcy, I. W.; Spielman, J. *Inorg. Chem.* **1967**, *6*, 1465. (b) Gaines, D. E.; Iornes, T. V. *J. Am. Chem. Soc.* **1967**, *89*, 3375. (c) Geanangle, R. A.; Shore, S. G. *J. Am. Chem. Soc.* **1967**, *89*, 6771.

(100) Corcoran, E. W.; Sneddon, L. G. *J. Am. Chem. Soc.* **1985**, *107*, 7446.

(101) Moody, D. C.; Schaeffer, R. O. *Inorg. Chem.* **1976**, *15*, 233–234.

(102) Corcoran, E. W.; Sneddon, L. G., pp 83–86 of ref 80.

(103) Tippe, A.; Hamilton, W. C. *Inorg. Chem.* **1969**, *8*, 464.

(104) Moody, D. C.; Schaeffer, R. O. *Inorg. Chem.* **1976**, *15*, 235.
(105) Greenwood, N. N.; Gysling, H. J.; McGinnety, J. A.; Owen, J. D. *J. Chem. Soc., Dalton* **1970**, 505. *J. Chem. Soc., Dalton* **1972**, 986.
(106) Huffman, J. C. Report No. 82210, Indiana University of Chemistry Molecular Structure Center.
(107) Getman, T. D.; Krause, J. A.; Niedenzu, P. M.; Shore, S. G. *Inorg. Chem.* **1989**, *28*, 1507.
(108) Tebbe, F. N.; Garrett, P. M.; Hawthorne, M. F. *J. Am. Chem. Soc.* **1966**, *88*, 607.
(109) (a) Stibr, B.; Plesek, J.; Hermanek, S., Chapter 3, pp 62–65 of ref 80. (b) Howarth, O. W.; Jasztal, M. J.; Taylor, J. G.; Wallbridge, M. G. H. *Polyhedron* **1985**, *4*, 1466.
(110) Kendall, D. S.; Lipscomb, W. N. *Inorg. Chem.* **1973**, *12*, 546.
(111) Sands, D. E.; Zalkin, A. *Acta Crystallogr.* **1962**, *15*, 410.
(112) Williams, R. E., Chapter 2, pp 67–68 of ref 1.
(113) (a) Schaeffer, R. O.; Tebbe, F. N. *J. Am. Chem. Soc.* **1963**, *85*, 2020. (b) Muller, J.; Paetzold, P.; Runsink, J.; Englert, U. *Chem. Ber.* In Press. (c) Kennedy, J. D.; Thornton-Pett, M.; Stibr, B.; Jelinek, T. *Inorg. Chem.* **1991**, *30*, 448.
(114) Brellochs, B.; Binder, H. *Angew. Chem., Int. Ed. Engl.* **1988**, *27*, 262.
(115) Shore, S. G., personal communication to R. E. Williams, August 1991.
(116) Masamune, S.; Sakai, M.; Kemp-Jones, A. V.; Nakashima, T. *Can. J. Chem.* **1974**, *52*, 855.
(117) Paine, R. T.; Parry, R. W. *Inorg. Chem.* **1975**, *14*, 689.
(118) Kodama, G.; Mitsuaki, K. *Inorg. Chem.* **1979**, *18*, 3302.
(119) Fratini, A. V.; Sullivan, G. W.; Denniston, M. L.; Hertz, R. K.; Shore, S. G. *J. Am. Chem. Soc.* **1974**, *96*, 3013.
(120) Shore, S. G.; et al.; see ref 5, p 5398.
(121) Hart, H.; Kazuya, M. *Tetrahedron Lett.* **1973**, *42*, 4133.
(122) Buehl, M.; Schleyer, P. v. R.; McKee, M. L. *Heteroatom Chem.* **1991**, *2*, 499.
(123) (a) Mangion, M.; Hertz, R. K.; Denniston, M. L.; Long, J. R.; Clayton, W. R.; Shore, S. G. *J. Am. Chem. Soc.* **1976**, *98*, 449. (b) Brellocks, B.; Binder, H. *Angew. Chem., Int. Ed. Engl.* **1988**, *27*, 262.
(124) Matteson, D. S.; Matteschei, P. K. *Inorg. Chem.* **1973**, *12*, 2472.
(125) (a) Williams, R. E. IMEBORON-III, Munchen-Ettal, 1976. (b) Williams, R. E.; Field, L. D.; IMEBORON-IV; Snowbird, UT, 1979 In *Boron Chemistry*; Parry, R. W., Kodama, G., Eds.; Pergammon Press: Oxford, 1980.
(126) Rasul, G.; Prakash, G. K. S.; Williams, R. E.; Kodama, G.; Parry, R. W. Detailed ab initio/IGLO/NMR results will be reported elsewhere.
(127) Paetzold, P.; Redenz-Stormans; Boese, R.; Buehl, M.; Schleyer, P. v. R. *Angew. Chem., Int. Ed. Engl.* **1990**, *29*, 1059.
(128) Cotton, F. A.; Kibala, P. A.; Wojtczak, W. A. *J. Am. Chem. Soc.* **1991**, *113*, 1462.
(129) The compound $((CH_3)_2N)_2B_4H_6$ was reported (of unknown structure) by Burg: Burg, A. B. *J. Am. Chem. Soc.* **1957**, *79*, 2129. We propose that the structure might be $((CH_3)_2N-H)_2B_4H_4$ or more generally $L_2B_4H_4$.
(130) (a) Rudolph, R. W.; Pretzer, W. R. *Inorg. Chem.* **1972**, *11*, 1974. (b) Rudolph, R. W. *Acc. Chem. Revs.* **1976**, *9*, 446.
(131) Sang, O. K.; Furst, G. T.; Sneddon, L. G. *Inorg. Chem.* **1989**, *28*, 2339.
(132) Once Shore had determined the correct structure of $B_{11}H_{14}^{-}$ (see ref 26) the ^{11}B and ^{1}H NMR data of How et al. (How, D. V.; Jones, C. J.; Wiersema, R. J.; Hawthorne, M. F. *Inorg. Chem.* **1971**, *10*, 2516) were reinterpreted by the original authors as well as several other groups to support the 481 configuration (Figure 48).
(133) Avdeef, A.; Raymond, K. N.; Hodgson, K. O.; Zalkin, A. *Inorg. Chem.* **1972**, *11*, 1083.